Tran-SET

Transportation Consortium of South-Central States

Solving Emerging Transportation Resiliency, Sustainability, and Economic Challenges through the Use of Innovative Materials and Construction Methods: From Research to Implementation

Use of Ultra-High-Performance Fiber-Reinforced Concrete (UHP-FRC) for Fast and Sustainable Repair of Pavements

Project No. 17STUTA03

Lead University: University of Texas at Arlington

Preserving Existing Transportation Systems

Final Report

December 2018

Disclaimer

The contents of this report reflect the views of the authors, who are responsible for the facts and the accuracy of the information presented herein. This document is disseminated in the interest of information exchange. The report is funded, partially or entirely, by a grant from the U.S. Department of Transportation's University Transportation Centers Program. However, the U.S. Government assumes no liability for the contents or use thereof.

Acknowledgments

The information regarding current pavement repair practice and design was provided by Dr. Romanoschi, Professor at the University of Texas at Arlington; Jean Gamarra, Program Manager/Civil Engineer for the Airport District Office (ADO) for Louisiana and New Mexico (LA/NM) in the Southwest Region (SW) at the Federal Aviation Administration (FAA); and Wayne Switzer; Supervisory General Engineer at Patuxent River Naval Air Station, Public Works. Their help is greatly appreciated.

TECHNICAL DOCUMENTATION PAGE

1. Project No.	2. Government Accession No.	3. Recipient's Catalog No.
17STUTA03		

4. Title and Subtitle	5. Report Date
Use of Ultra-High-Performance Fiber-Reinforced Concrete (UHP-FRC) for Fast and Sustainable Repair of Pavements	Dec. 2018
	6. Performing Organization Code
7. Author(s) PI: Shih-Ho Chao https://orcid.org/0000-0003-2679-7364 GRA: Ashish Karmacharya https://orcid.org/0000-0001-7517-7693	**8. Performing Organization Report No.**
9. Performing Organization Name and Address Transportation Consortium of South-Central States (Tran-SET) University Transportation Center for Region 6 3319 Patrick F. Taylor Hall, Louisiana State University, Baton Rouge, LA 70803	**10. Work Unit No. (TRAIS)** **11. Contract or Grant No.** 69A3551747106
12. Sponsoring Agency Name and Address United States of America Department of Transportation Research and Innovative Technology Administration	**13. Type of Report and Period Covered** Final Research Report May 2017 – May 2018 **14. Sponsoring Agency Code**

15. Supplementary Notes

Report uploaded and accessible at: Tran-SET's website (http://transet.lsu.edu/)

16. Abstract

This research presents a new methodology, which enables streets, roads, highways, bridges, and airfields to use an advanced fiber-reinforced concrete material, which can delay or prevent the deterioration of these transportation infrastructure when subjected to traffic and environmental loadings. The major problem of concrete is its considerable deterioration and limited service life due to its brittleness and limited durability. As a result, it requires frequent repair and eventual replacement, which consumes more natural resources. Ultra-high-performance fiber-reinforced concrete (UHP-FRC) introduces significant enhancement in the sustainability of concrete structures due to its dense microstructure and damage-tolerance characteristics. These characteristics can significantly reduce the amount of repair, rehabilitation, and maintenance work, thereby giving the transportation infrastructure a longer service life. This research addresses the strong need to develop fast and sustainable UHP-FRC materials for pavement repair that can be easily cast onsite without special treatments. This avoids any major changes to current concrete production practice and accelerates the use of UHP-FRC materials. This research investigated a new method for concrete repair by combining precast UHP-FRC panels with a small quantity of cast-in-place UHP-FRC for pavement repair without any dowel bars. In this method, a precast UHP-FRC panel is used along with cast-in-place UHP-FRC. The vertical repair surfaces of the existing concrete are roughened on site. The outer edges of the UHP-FRC precast panel are roughened before they are brought to the site (no dowel bars are needed). The depth of the precast UHP-FRC panel is the same as the existing pavement thickness. Only a small cast-in-place UHP-FRC joint (one to two inches wide) is done onsite. The roughened precast UHP-FRC panel is placed in the repair area and cast-in-place UHP-FRC is cast into the joint. Experimental results showed that using a roughened surface (up to about CSP 5) provides a very large bond resistance, which is enough to prevent faulting.

17. Key Words	18. Distribution Statement
UHP-FRC, pavement, repair	No restrictions.

19. Security Classif. (of this report)	20. Security Classif. (of this page)	21. No. of Pages	22. Price
Unclassified	Unclassified	70	

Form DOT F 1700.7 (8-72) **Reproduction of completed page authorized.**

SI* (MODERN METRIC) CONVERSION FACTORS

APPROXIMATE CONVERSIONS TO SI UNITS

Symbol	When You Know	Multiply By	To Find	Symbol
		LENGTH		
in	inches	25.4	millimeters	mm
ft	feet	0.305	meters	m
yd	yards	0.914	meters	m
mi	miles	1.61	kilometers	km
		AREA		
in^2	square inches	645.2	square millimeters	mm^2
ft^2	square feet	0.093	square meters	m^2
yd^2	square yard	0.836	square meters	m^2
ac	acres	0.405	hectares	ha
mi^2	square miles	2.59	square kilometers	km^2
		VOLUME		
fl oz	fluid ounces	29.57	milliliters	mL
gal	gallons	3.785	liters	L
ft^3	cubic feet	0.028	cubic meters	m^3
yd^3	cubic yards	0.765	cubic meters	m^3
		NOTE: volumes greater than 1000 L shall be shown in m^3		
		MASS		
oz	ounces	28.35	grams	g
lb	pounds	0.454	kilograms	kg
T	short tons (2000 lb)	0.907	megagrams (or "metric ton")	Mg (or "t")
		TEMPERATURE (exact degrees)		
^oF	Fahrenheit	5 (F-32)/9 or (F-32)/1.8	Celsius	^oC
		ILLUMINATION		
fc	foot-candles	10.76	lux	lx
fl	foot-Lamberts	3.426	candela/m^2	cd/m^2
		FORCE and PRESSURE or STRESS		
lbf	poundforce	4.45	newtons	N
lbf/in^2	poundforce per square inch	6.89	kilopascals	kPa

APPROXIMATE CONVERSIONS FROM SI UNITS

Symbol	When You Know	Multiply By	To Find	Symbol
		LENGTH		
mm	millimeters	0.039	inches	in
m	meters	3.28	feet	ft
m	meters	1.09	yards	yd
km	kilometers	0.621	miles	mi
		AREA		
mm^2	square millimeters	0.0016	square inches	in^2
m^2	square meters	10.764	square feet	ft^2
m^2	square meters	1.195	square yards	yd^2
ha	hectares	2.47	acres	ac
km^2	square kilometers	0.386	square miles	mi^2
		VOLUME		
mL	milliliters	0.034	fluid ounces	fl oz
L	liters	0.264	gallons	gal
m^3	cubic meters	35.314	cubic feet	ft^3
m^3	cubic meters	1.307	cubic yards	yd^3
		MASS		
g	grams	0.035	ounces	oz
kg	kilograms	2.202	pounds	lb
Mg (or "t")	megagrams (or "metric ton")	1.103	short tons (2000 lb)	T
		TEMPERATURE (exact degrees)		
^oC	Celsius	1.8C+32	Fahrenheit	^oF
		ILLUMINATION		
lx	lux	0.0929	foot-candles	fc
cd/m^2	candela/m^2	0.2919	foot-Lamberts	fl
		FORCE and PRESSURE or STRESS		
N	newtons	0.225	poundforce	lbf
kPa	kilopascals	0.145	poundforce per square inch	lbf/in^2

TABLE OF CONTENTS

LIST OF FIGURES

LIST OF TABLES

ACRONYMS, ABBREVIATIONS, AND SYMBOLS

AASHTO	American Association of State Highway and Transportation Officials
ASTM	American Society for Testing and Materials
CELB	Civil Engineering Laboratory Building
CRCP	Continuously Reinforced Concrete Pavement
CSP	Concrete Surface Profile
DAQ	Data Acquisition
FAA	Federal Aviation Administration
FHWA	Federal Highway Administration
HMA	Hot Mix Asphalt
ICRI	International Concrete Repair Institute
JPCP	Jointed Plain Concrete Pavement
JRCP	Jointed Reinforced Concrete Pavement
LVDT	Linear Variable Differential Transformer
MAST	Multi-Axial Sub-assemblage Testing
PC	Plain Concrete
SST	Slant Shear Test
TxDOT	Texas Department of Transportation
UHP-FRC	Ultra-High-Performance Fiber-Reinforced Concrete
UTA	University of Texas at Arlington

EXECUTIVE SUMMARY

Durability issues with conventional plain concrete has led to significant higher life-cycle costs in comparison to construction costs. Repair, replacement and maintenance of the existing structures are estimated to increase by 30% owing to the change in climatic conditions and transportation demand changes.

Ultra-high-performance fiber-reinforced concrete (UHP-FRC) with its high compressive strength and excellent environmental resistance and durability provides a solution to make the infrastructure more economical and sustainable. UHP-FRC has a high early strength gain which drastically reduces the downtime of traffic after pavement repair. Also, the presence of fibers imparts tensile cracking resistance, post-cracking strength, ductility and energy absorption capacity.

The first phase of this research focused on the material development needed to tailor the UHP-FRC previously developed at UT-Arlington for the needs of pavement construction and repair. In the second phase, a slant shear test was used to quantify the interface shear capacity of existing plain concrete and UHP-FRC repair. Although simple, slant shear test overestimates the shear capacity due to the presence of a frictional force developed as a result of a normal component of the applied load. As a result, in the third phase, a new punch test was developed. This punch test incorporates a specimen much like an actual pavement repair situation with vertical interfaces between the existing plain concrete and the repair materials for accurate determination of the interface shear capacity. The test data indicated that the interface shear strength of UHP-FRC is much higher than that of conventional concrete.

Test results for both the slant shear test and punch test indicated that the dowel bars do not participate in the load transfer at peak load. A certain value of vertical deformation after the initial slip is required before the dowel bars can start accepting load. Hence, it is possible to remove the dowel bars from the pavement repair and use a roughened interface to enhance the bond between the interfaces. This significantly reduces the repair time and makes the repair process simple and convenient.

In the punch test, a new idea of pavement repair was tested for the UHP-FRC: A precast UHP-FRC panel was used for the full depth repair and the joint was sealed using cast-in-place UHP-FRC. By using this approach, good quality can be achieved using the precast panel. Furthermore, the subsequent reduction of cast-in-place UHP-FRC not only minimizes the volume but also reduces the on-site time. This makes the process very convenient.

IMPLEMENTATION STATEMENT

Throughout this research, the research team has kept communication open for input and exchange of ideas as well as discussion on progress with the City of Bedford, Texas, the Federal Aviation Administration (FAA) and Dallas-Fort Worth International Airport in Texas, A pilot implementation was conducted in the City of Bedford. See Section “Field Installation” for more details. For the Dallas-Fort Worth International Airport apron and taxiway pavement replacement, a proof-of-concept test will be done in early 2019. To disseminate the research results, our paper has been accepted and we will present the research findings at the 2019 ASCE International Airfield and Highways Pavements Conference, which is one of the most important conferences for transportation pavements. The audiences are from airports, local cities, consultants, and DOTs. The results will be also presented at the 2019 Tran-SET Conference in Texas.

1. INTRODUCTION

Statistical data shows that in industrially developed countries, about 50% of total construction costs are related to repair, replacement, and maintenance of existing structures that have deteriorated or been damaged by environmental stress, structural loading, or other effects *(1)*. Durability issues of structures can lead to a significantly higher life-cycle cost in comparison to the initial construction cost. Transportation infrastructure can quickly deteriorate due to overloading by increasing traffic, climate change, and other environmental loads. For example, climate change such as summer heat waves, droughts, and flooding can have major impacts on the pavement maintenance and rehabilitation costs. These extreme events are likely to occur in greater frequency and intensity in the future as the global temperature continues to rise. Rainfall changes can alter moisture balances and influence pavement deterioration. In addition, temperature can also affect the aging of bitumen resulting in an increase in cracking of the pavement surface, with a consequent loss of waterproofing. The result is that surface water can enter the pavement causing rapid loss of surface condition. Changes in temperature and rainfall patterns can interact when higher temperatures increase cracking. Pavement maintenance and rehabilitation budget can considerably increase in the coming years considering both the influences of climate change and transport demand changes. Deficiencies in conventional concrete and its subsequent impact on the environment calls for a much more durable material that will last longer under environmental stress, thereby contributing to the conservation of natural resources and the protection of the ecosystem.

Many solutions have been proposed for enhancing the sustainability of concrete, and the use of ultra-high-performance fiber-reinforced concrete (UHP-FRC) is a promising one. UHP-FRC has recently attracted the attention of researchers and practitioners not only because of its high compressive strength but also because of its excellent environmental resistance *(2)*. The porous nature of conventional concrete can be improved by reducing dimensions of microcracking (or defects) in the concrete resulting in enhanced compressive strength *(3)* and delayed liquid ingress. This is achieved in UHP-FRC through a very low water to cementitious material ratio (w/cm) and dense particle packing, which leads to almost no shrinkage or creep (which significantly reduces prestress losses and long-term deformations). Furthermore, the addition of fibers (typically 2 to 4 percent by volume of concrete) not only improves the brittleness of concrete by increasing the tensile cracking resistance, post-cracking strength, ductility, and energy absorption capacity (Figure 1), but also improves the ability of concrete to resist negative environmental effects. Its high-early strength and durability allow for fast reopening of traffic to areas previously closed by repair and fewer detours due to less need for future repairs.

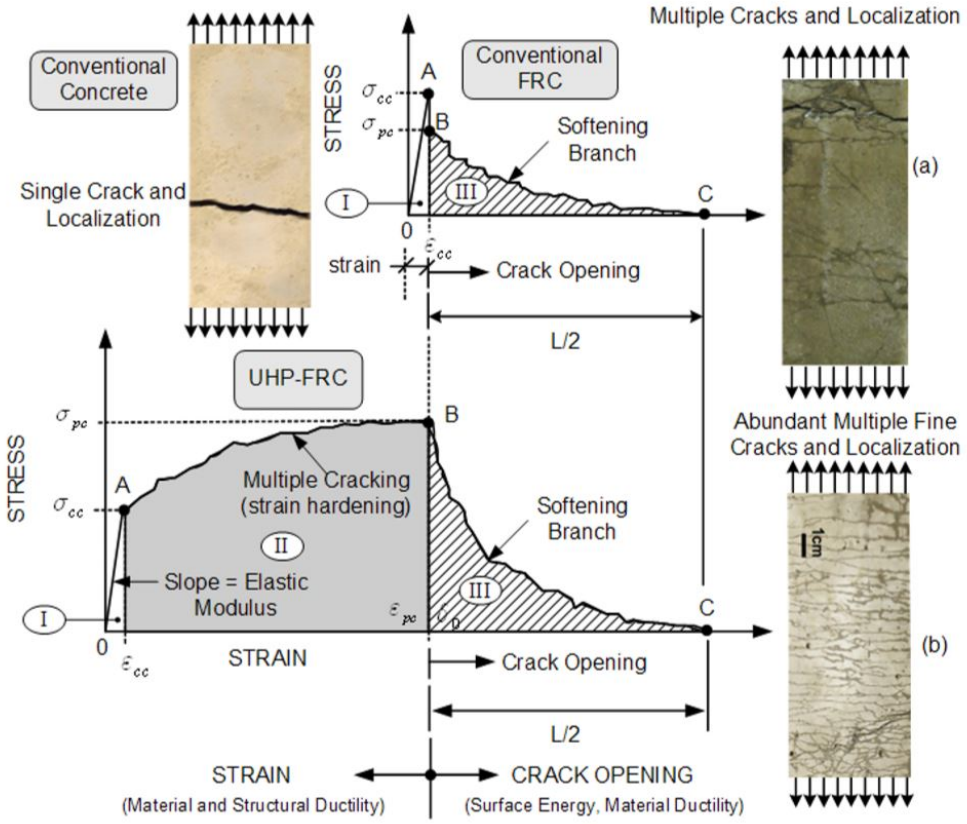

Figure 1. Ductile (tensile strain-hardening) behavior of UHP-FRC (4).

This project offers a new methodology, which will enable the transportation infrastructure to use an advanced fiber-reinforced concrete material, UHP-FRC, that can delay or prevent the deterioration of transportation infrastructure when subjected to traffic and environmental loadings. The major problem of concrete is the considerable deterioration and consequent repair work needed due to its brittleness and limited durability. The consequence of concrete deterioration and short service life requires frequent repair and eventual replacement, which consumes more natural resources.

1.1. Background

1.1.1. Pavement Types

Rigid pavement and flexible pavement are two different types of pavements. Flexible pavements deflect or flex under loading. They are surfaced by bituminous or asphalt materials. Depending on the volume of traffic, flexible pavements can be either in the form of pavement surface treatments for lower traffic volume or hot-mix asphalt (HMA) surface courses for higher traffic volume. In this type of pavement, the load is distributed over a small area due to its flexible nature. Load is transferred to the subgrade by the combination of different layers.

Rigid pavements are firm and do not deform under loading. They exhibit higher elastic modulus than the flexible pavements. They are made up of a plain concrete (PC) surface course and might have steel reinforcement bars to reduce or eradicate the joints. Due to their stiff

nature, they distribute the load over a wide area of subgrade. Most of the structural capacity is provided by the concrete slab.

Broadly, rigid pavements can be classified into three different types: jointed plain concrete pavement (JPCP), continuously reinforced concrete pavement (CRCP) and jointed reinforced concrete pavement (JRCP) as shown in Figure 2. They are discussed below:

Continuously Reinforced Concrete Pavement (CRCP): Continuously reinforced concrete pavement (CRCP) is comprised of continuous, longitudinal reinforcing steel of about 0.6–0.7 percent of the cross-section pavement area with the reinforcements placed at mid-depth. No. 5, and No. 6 bars are generally used. Transverse joints are absent in this type of rigid pavement. In the new CRCP, restraint stresses and tensile stresses are developed because of volumetric changes due to cement hydration, thermal effects and external drying. These stresses increase rapidly in the early stages. This causes full depth transverse cracks dividing the pavement into short, individual slabs. The continuous reinforcements act as an internal restraint in CRCP *(5)*. The reinforcement steel bars permit the formation of contraction cracks at small intervals but is designed to limit the cracks to 0.02 inches (0.5 mm). This aids in the transfer of load to the adjacent slabs through aggregate interlock and prevents spalling and water penetration.

Jointed Plain Concrete Pavement (JPCP): Jointed plain concrete pavement (JPCP) consists of plain concrete slabs without any reinforcing steel. It uses contraction joints for crack control. The transverse joint spacing is determined from temperature and moisture stress considerations, and is typically limited to 20 ft (6.1 m). The spacing is selected to prevent any intermediate cracking between the joints. The joint spacing is typically between 12 ft (3.7 m) and 20 ft (6.1 m). The spacing is limited by the nature of the concrete. Due to the limited tensile capacity of plain concrete, slabs greater than 20 ft usually break in the middle. The load transfer at the joint takes place from aggregate interlock and the dowel bar action of the smooth bars *(6)*. Unlike the CRCP where transverse cracks are created throughout the slab due to the developed tensile stresses, the location of cracks are directed using timely sawing in JPCP.

Jointed Reinforced Concrete Pavement (JRCP): Jointed reinforced concrete pavement (JRCP) consists of concrete pavement reinforced with wire mesh reinforcement of about 0.2% of the cross-sectional area of the concrete *(5)*. It uses contraction joints and reinforcing steel for crack control. The cracking due to the restraint stresses is limited by the reinforcing steel or the steel meshes. The interval for the transverse contraction joints is longer than for JPCP and ranges from 25 ft (7.6 m) to 50 ft (15.2 m). Load transfer is achieved in the transverse joints by means of dowel bars *(6)*.

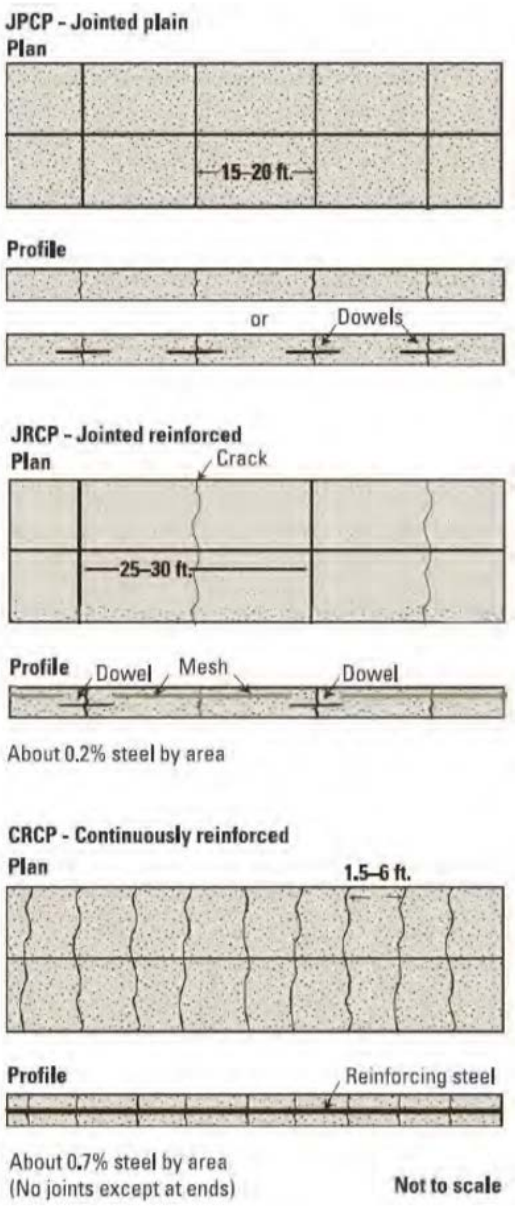

Figure 2. Three common rigid pavement types (5).

1.1.2. Rigid Pavement Rehabilitation Techniques

Major rehabilitation activities are defined as "*any work that is undertaken to significantly extend the service life of an existing pavement through the principles of resurfacing, restoration, and/or reconstruction*." *(7)*. The first step of the rehabilitation process is the evaluation of the pavement condition. In this phase, the problems existing in the pavement are identified. The types and the causes of the distress and the level of deterioration in the pavement is determined. The major factors which need to be considered during the consideration of major rehabilitation strategies are as follows *(7)*:

- Selection of a major rehabilitation category that may or may not involve an overlay (resurfacing).

- Decision to use new or recycled materials or a combination of both.
- Decision choosing the type of rehabilitation method to be employed which includes full reconstruction, partial reconstruction, a full overlay or a combination of reconstruction and overlay.
- Determination of the optimum rehabilitation technique through life-cycle cost analysis of several possible rehabilitation methods.

Depending on the joint/crack distress seen, the following repair and preventive methods can be adopted for rehabilitation purposes:

Table 1. Possible repair and preventive methods for different kinds of distresses for rigid pavements*.

Joint/Crack distress	#	Repair Methods	#	Preventive Methods
Pumping	1	Subseal	1	Reseal joints
			2	Restore load transfer
			3	Subdrainage
			4	Edge support (PCC shoulder/edge beam)
Faulting	1	Grind	1	Subseal
	2	Structural overlay	2	Reseal joints
			3	Restore load transfer
			4	Subdrainage
			5	Edge support
Slab cracking	1	Full-depth repair	1	Subseal loss of support
	2	Replace/recycle lane	2	Restore load transfer
			3	Structural overlay
Joint or crack spalling	1	Full-depth repair	1	Reseal joints
	2	Partial-depth repair		
Blow-up	1	Full-depth repair	1	Pressure relief joint
			2	Resealing joints/cracks
Punchouts	1	Full-depth repair	1	Polymer or epoxy grouting
			2	Subseal loss of support
			3	Rigid shoulders

*From AASHTO Design Guide for Design of Pavement Structures, Vol. 1, Table 4.1 *(8)*.

Among the different possible major rehabilitation techniques, this research looks into the full-depth pavement repair of rigid pavements; jointed plain concrete pavement (JPCP) and continuously reinforced concrete pavement (CRCP) shown in Figure 3.

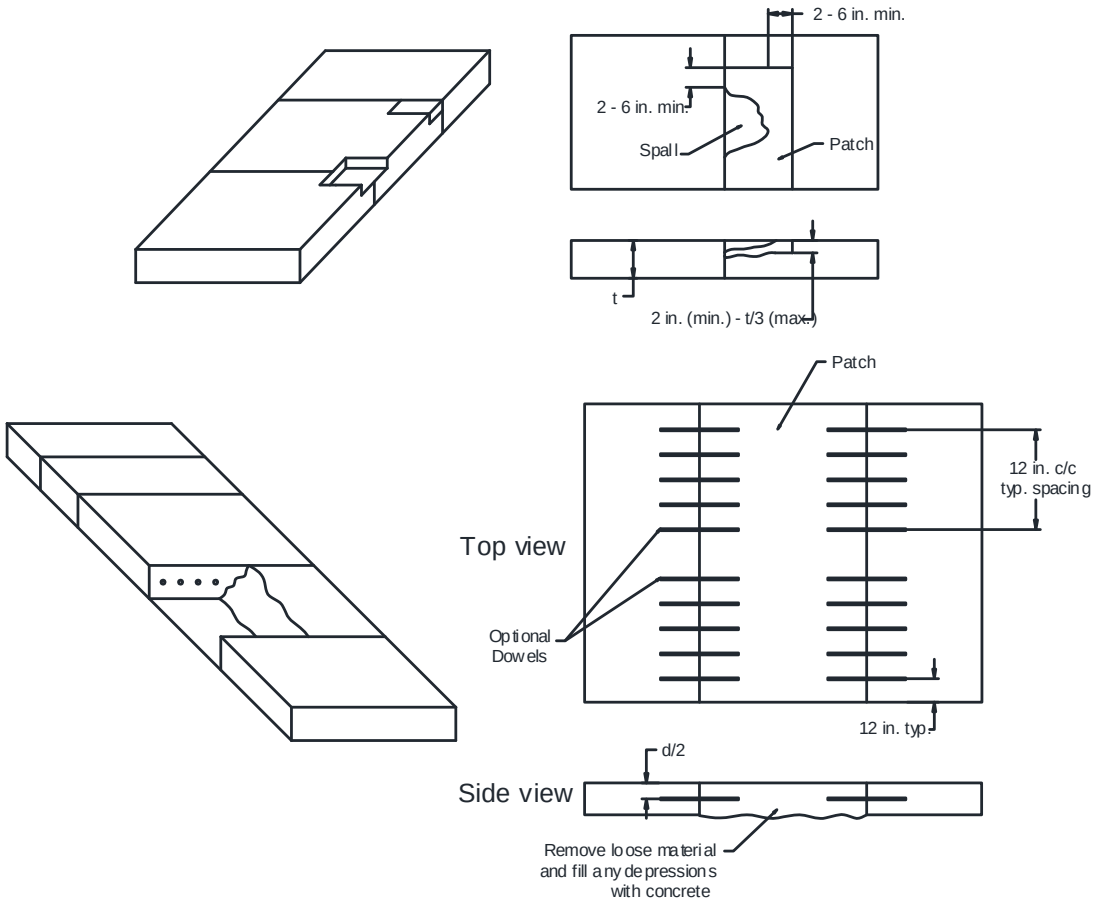

Figure 3. Partial and full-depth patches.

Full-Depth Repair: This repair method is a rehabilitation technique that is commonly used for the restoration of structural integrity and provides a smooth vehicular movement in the pavement. This is done for the full-depth and full-width across the lane. Transverse cracks, which extend throughout the depth of the slab, need to be treated with full-depth repair. The full-depth cracks are created due to temperature/moisture variations and wheel-load stresses. Shattered slabs and corner breaks also require full-depth repair. These distresses are caused due to pavement design issues and construction issues. This method of pavement rehabilitation can be used in all types of pavement.

Portland cement concrete is used for full-depth repair purposes. Depending on the project requirements, it is possible to achieve very early opening time. By changing the constituents of the concrete mixture, very high early strength can be achieved. This involves reducing the water to cement ratio, using well-graded aggregates, accelerating admixtures, and increasing the cement content.

Full-Depth Repair of Jointed Concrete Pavement: The pavement joint is a major factor which influences the performance of jointed concrete pavement. Deficient joints with insufficient load transfer generated distress such as spalling, rocking of the patch, faulting and corner breaks. The transfer of load across the patched joint interface can be achieved by one or a combination of tie bars, dowel bars, undercutting and aggregate interlock. In the case of

jointed concrete pavements, full-depth repair is suitable for distresses such as blow-ups, corner breaks, durability "D" cracking (caused by the freezing and thawing aggregate problem), and distress caused by insufficient load transfer across the joint and excessive spalling.

Full-depth Repair of Continuously Reinforced Concrete Pavement: This involves cast-in-place concrete repair requiring the full-depth repair of CRCP. For adequate transfer of load, the reinforcing steel must be extended for sufficient length into the repair. It should be tied or welded to the reinforcement added in the repair for adequate bond development; moreover, the repair face needs to be vertical. Full-depth repair is applicable to CRCP in cases such as blow-ups, punchouts, durability "D" cracking, and construction joint problems.

Full-depth Repair Procedure: The procedure of the full-depth pavement repair is described below *(9, 10)*:

1. The first step for full depth repair is identifying the location of distress and selection of boundaries. It should include all the areas showing distress including the ones not visible from the surface to avoid pavement failures in the future. Appropriate load transfer across the repair joints is essential to ensure the performance of the repair.
2. Then, a diamond-blade saw is used to cut full depth transverse cuts to isolate the deteriorated concrete. The deteriorated concrete is then removed using either the lift-out method or the breakup method. Among them, the lift-out method is favored as it is quick and does not disturb the subgrade.
3. After that the repair area is prepared. Any disturbed base, subbase and subgrade materials should be removed and replaced with concrete. The repair area should be free of moisture before new materials are added.
4. Load transfer across the repair joint is fundamental. The depth of the holes should be 10 in. *(11)* to make sure sufficient bond develops between concrete and the dowel bars. The holes should be cleaned properly and absent of moisture, dust and oil. The holes are then filled with epoxy and dowels are inserted. At least four dowel bars should be used for each wheel path. For CRCP, continuity of the longitudinal reinforcements at the transverse joint must be sustained. To maintain continuity, a minimum of 33 times the diameter of the transverse reinforcing steel *(11)* should be provided as the embedment length to prevent reinforcement pullout.
5. The next step is the pouring of the concrete. Hand vibrators are used to consolidate the concrete. The surface is then textured comparable to the surrounding concrete. The concrete is covered properly to prevent the loss of moisture. The concrete must be properly cured to avoid map cracking due to excessive evaporation and large temperature gradient.
6. Finally, the transverse and longitudinal joints are sawed, formed, and then sealed. The objective of doing so is to reduce spalling and infiltration of water.
7. The pavement can be reopened for traffic when the concrete reaches a compressive strength of 2000 lb/in^2 (13,780 kPa).

Partial-Depth Repair: Surface defects and shallow joint spalling is treated by partial-depth pavement repair. This method of repair is selected when the distress does not extend through the full-depth of the slab and the load transfer mechanisms across the joint are operative. Partial-depth repair is used to deal with distress in the pavement such as localized scaling, early stages of "D" cracking and low spalling.

The choice of material for the partial-depth repair relies primarily on the required opening time of the project. The curing time, ambient temperature, cost and performance and the repair size are also important factors in the determination of materials used. Partial-depth repair materials can broadly be classified into cementitious, polymer-based and bituminous materials. Among them cementitious materials, which includes the Portland cement concrete, is the most commonly used. As with the full-depth repair, the constituents can be altered to obtain the required properties. However, it exhibits similar durability issues.

Procedure for Partial-Depth Repair: Partial-depth pavement repair encompasses the following steps *(10)*:

1. The first step is to identify the extent of distress and the limit of repair. The area is marked to include all deterioration.
2. Then, the deteriorated concrete is removed. The perimeter of the marked area is saw-cut to a minimum depth of 1-1/2 inches, and then the damaged concrete is chipped off to uncover sound concrete within.
3. To ensure a good bond development between the old concrete and the new concrete interface, the old concrete exposed surface should be cleaned with water to remove any dust before casting the new concrete.
4. After that, the repair materials are placed. Precautions needed to ensure a good bond development should be adopted. In the case of ready-mix concrete, the repair surface should be saturated with water without ponding before the concrete is placed.
5. Finally, the surface is finished to bring the repair surface to the same elevation as the pavement surface. The texture of the repaired surface is also matched to the surrounding concrete. The repaired concrete should be properly cured to prevent excessive volume changes due to drying shrinkage.

1.1.3. Precast Concrete Pavement Repair at Full-depth

Precast concrete pavement uses precast panels for accelerated pavement repair and rehabilitation. The precast panels used in this method of concrete repair are cast off site, transported to the repair site and installed. Because of being prepared in a controlled environment with better curing conditions, the concrete quality of the precast slab is significantly better than the cast-in-place concrete. Moreover, this method of concrete repair needs minimum curing time before it can be opened for traffic significantly reducing the opening time.

Precast concrete pavement repair is carried out for the full-lane replacement of fractured slab and for full-depth repair of cracked slabs or slabs with deteriorated joints. The repair is always carried out for the full-lane width. In one method of repair, the dowel bars are installed in the precast concrete panel. Slots for the dowel bars are cut into the existing pavement. The precast panel is put in place and the slots are filled with fast-setting patching material. The second method is similar to the method of cast-in-place, full-depth repair; the dowel bars are fixed in the existing pavement by the process of drilling and grouting with epoxy. Slots are fabricated in the precast concrete panel in the transverse side on the bottom side. The precast panels are then put in place and the slots and the perimeter joint is filled with fast setting grout.

1.1.4. Comparison of Rigid Pavement Repair Alternatives

The pavement design alternatives can broadly be categorized into three types: rigid pavements using conventional mix concrete, rigid pavements using rapid-setting concrete and rigid pavements using precast panels. Choice of the alternatives depends on the requirements of the project. It also depends on other parameters such as the available curing time, the ambient temperature, the material cost and the desired performance. Each of the three types of pavement mentioned above has its own advantages and disadvantages which must be considered with respect to the project requirements before making the choice for a certain type. The pros and cons of each alternative are discussed below *(12)*:

Conventional Rigid Pavement Repair: The primary advantage of conventional rigid pavement is its high final strength. Conventional concrete has been in use for a very long time. As a result, contractors and workers have the tools, equipment and necessary experience required for working with conventional concrete. Conventional concrete has well defined specification, testing methods and proven design ensuring the quality of the mix. Compared to rapid set and precast panels, it is easier to work with this type of concrete and the materials are readily available in the market. Also, the cost estimates can be done with a reasonable degree of accuracy. The cost of using conventional mix is lower over using rapid-set and precast panels. It results in a pavement with low maintenance and longer life span compared to the other two.

The major disadvantage of this rigid pavement is a longer reopening time. This mix requires considerable construction as well as curing time, which leads to a very long downtime. Also, if the concrete used for the repair does not meet the determined specification, the concrete has to be removed and placed again.

Accelerated Early Strength Gaining Rigid Pavement Repair: In this type of Portland cement concrete (PCC) the concrete mixture is tailored to obtain very high early strength. This involves reducing the water to cement ratio, using well-graded aggregate, accelerating admixtures and increasing the cement content. The early strength gain is mostly dependent in the properties of the cement and the additives used. The high early strength provides the required compressive strength within a few hours. This allows for the opening of the pavement for driving with minimum downtime.

Although the reduced downtime is a huge benefit, the cost of using this type of concrete is high. It has a lower final strength. Mixes for high early-strength concrete present problems such as poorly formed air voids, less homogeneous paste and increased microcracking, alkali silica reaction (ASR), and a high degree of scaling *(13)*. This affects the long-term serviceability of the pavement and imparts a shorter life span than the regular conventional mix. A very low setting time of the concrete poses many difficulties in the use of this alternative. It requires a larger work force and precise scheduling. Also, inexperienced contractors not accustomed to working with this type of concrete make it arduous. The concrete has low workability and has an increased safety risk to workers because of the caustic nature of some accelerants. If the specifications are not met, the concrete has to be removed and redone which takes additional time and money.

Precast Rigid Pavement Repair: Using precast slabs permits rapid repair of pavement. The panels are fabricated off site in a controlled environment. This ensures good quality of concrete. The strength can further be improved by prestressing them.

Despite the merits, using precast panels for pavement repair poses some challenges. The cost of using precast panels is high. Inexperience of the contractors and workers with this type of pavement repair makes the process arduous. Also, transporting the precast panels from the precast plant to the site and positioning of the precast panels in place is difficult. The edges of the precast panels are likely to get damaged and this process of repair may require power grouting or lifting screw jacks *(14)*.

1.1.5. Characteristics of UHP-FRC

In a prior National Science Foundation-sponsored research project, the research team developed a highly flowable UHP-FRC mix by using currently available materials on the U.S. market. FRC was invented many decades ago; however conventional FRC only enhances the post-cracking ductility and its compressive strength is close to that of plain concrete (3 to 5 ksi). In other words, conventional FRC does not change the micro-structure of concrete but just the tensile capacity after concrete cracks. On the other hand, UHP-FRC's compressive strength is about 22–30 ksi (six times higher than conventional concrete) with a post-cracking tensile strain up to 0.6% without strength degradation. The one-day strength was approximately 12 ksi, which is more than twice that of the ultimate long-term strength of conventional concrete.

UHP-FRC has very high durability due to its dense microstructure *(15)*. Micro high-strength steel fibers were incorporated in the concrete mix to enhance its ductility and toughness. The excellent flowability of UHP-FRC was achieved by introducing a pozzolanic material (fly ash), which has a spherical shape. Its shape allows all the particles to roll over thereby increasing the flowability during the mixing state. The scientific basis of this invention is due to the fact that the void (or defect) dimensions and entrapped air are critical factors in determining concrete strength. The voids can be minimized by high packing density, induced by combined mixing of big- and small-sized particles, e.g., coarse and fine sands, cement, glass powder, and silica fume, to achieve ultra-high compressive strength. This approach is based on the fundamental particle-stacking theory, as briefly illustrated by Figure 4 *(16)*. Filling the interstitial voids with smaller particles can increase the packing density of the primary particles. There are two different ways to fill these voids—with a single large particle or with many small particles. In our approach, both void filling methods were combined to reach the highest concrete strength. Therefore, the combined particles are a primary particle (biggest size particle), a secondary small particle (filling voids in the middle of primary particles) and micro-sized particles. The void size was further reduced by reducing the water to a cementitious materials ratio down to about 0.2. A high-range water reducer was used to assist flowability during the mixing process. Because the process simply relies on particle packing and chemical admixture, no special treatment and mixing technique is needed to produce UHP-FRC; hence, it is suitable not only for precast but also on-site casting applications. The high compressive/tensile ductility, and excellent flowability have been experimentally verified as shown in Figure 5.

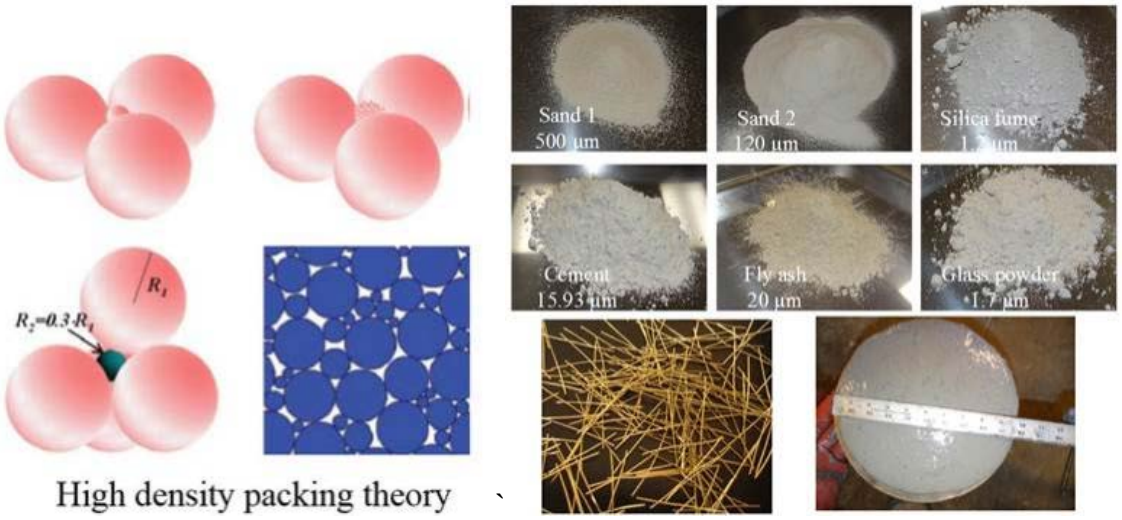

Figure 4. Fundamental concept of UHP-FRC and materials (16).

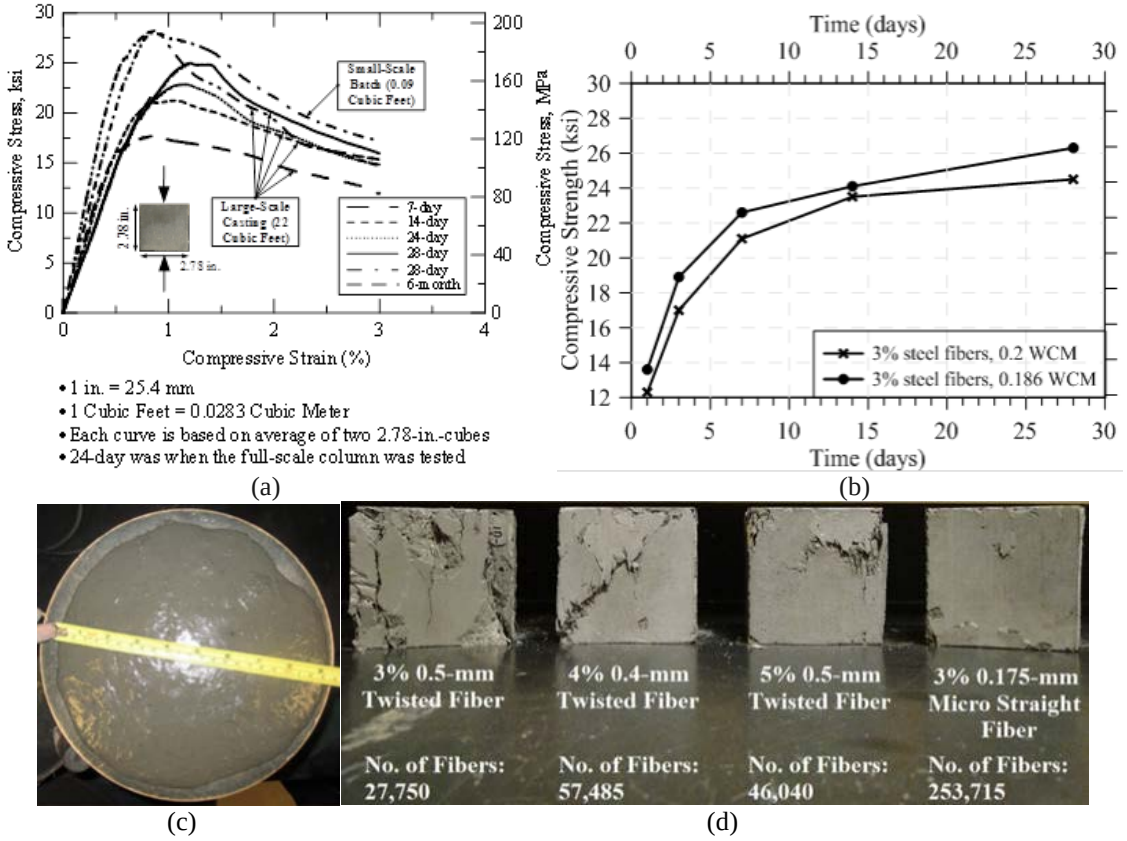

Figure 5. Features of UHP-FRC used for this study: (a) compressive stress-strength curves, (b) compressive strength development versus time, (c) flowability, and (d) improved compressive ductility with 3% micro straight steel fibers *(16)*.

UHP-FRC was developed by changing the porous nature of conventional concrete through reducing dimensions of microcracking (or defects) in the concrete. This is achieved in UHP-

FRC through a very low water to cementitious materials ratio (0.18 to 0.25) and a dense particle packing *(16)*, which leads to almost no shrinkage or creep, making it very suitable for concrete members under long-term compression. The consequences of a very dense microstructure and low-water ratio results in enhanced compressive strength and delayed liquid ingress. Furthermore, the addition of steel or synthetic fibers improves the brittle nature of concrete by increasing the tensile cracking resistance, post-cracking strength, ductility, and energy absorption capacity. In terms of corrosion resistance, research has indicated that UHP-FRC has a much greater durability than conventional concrete due to its very dense microstructure *(2)*. This dense microstructure impedes the conductive chloride ions from coming into direct contact with the steel reinforcing bars, which protects the reinforcing bars from corrosion. Table 2 provides a comparison between typical conventional concrete and UHP-FRC.

Table 2. Comparison of typical conventional concrete and UHP-FRC (UT Arlington test data except Rapid Chloride Penetration Test).

Properties of Concrete	Conventional Concrete	UHP-FRC
Ultimate Compressive Strength	< 8,000 psi (55 MPa)	18,000 to 30,000 psi (124 to 207 MPa)
Early (24-hour) compressive strength	< 3000 psi (21 MPa)	10,000 – 12,000 psi (69 to 83 MPa)
Flexural Strength	< 670 psi (4.6 MPa)	2,500 to 6,000 psi (17 to 41 MPa)
Shear strength	< 180 psi (1.2 MPa)	> 600 psi (4.1 MPa)
Direct Tension	< 450 psi (3 MPa)	up to 1,450 psi (10 MPa)
Rapid Chloride Penetration Test *(15)*	2000-4000 Coulombs passed	Negligible (< 100 Coulombs passed)
Ductility	Negligible	High ductility
Ultimate Compressive Strain, ε_{cu}	0.003	0.015 to 0.03
Confining	Negligible	High confining capability

1.2. Literature Review

1.2.1. Prior UHP-FRC Research

In a prior NSF research, UHP-FRC was used in a full-scale earthquake-resistant column. The high toughness and strength of the UHP-FRC was utilized and the operation successfully accomplished mixing and pouring at a 1-cubic yard scale, demonstrating applications for potential large-scale construction (Figure 6). The column was constructed at University of Texas at Arlington's (UTA) Civil Engineering Lab Building (CELB) and transported by a flatbed truck to the Multi-Axial Sub-assemblage Testing (MAST) facility at the University of Minnesota for testing. The testing results are shown in the Figure 7 below. UHP-FRC column had extremely high damage tolerance capability as compared to conventional reinforced concrete columns when subjected to severe earthquake motions.

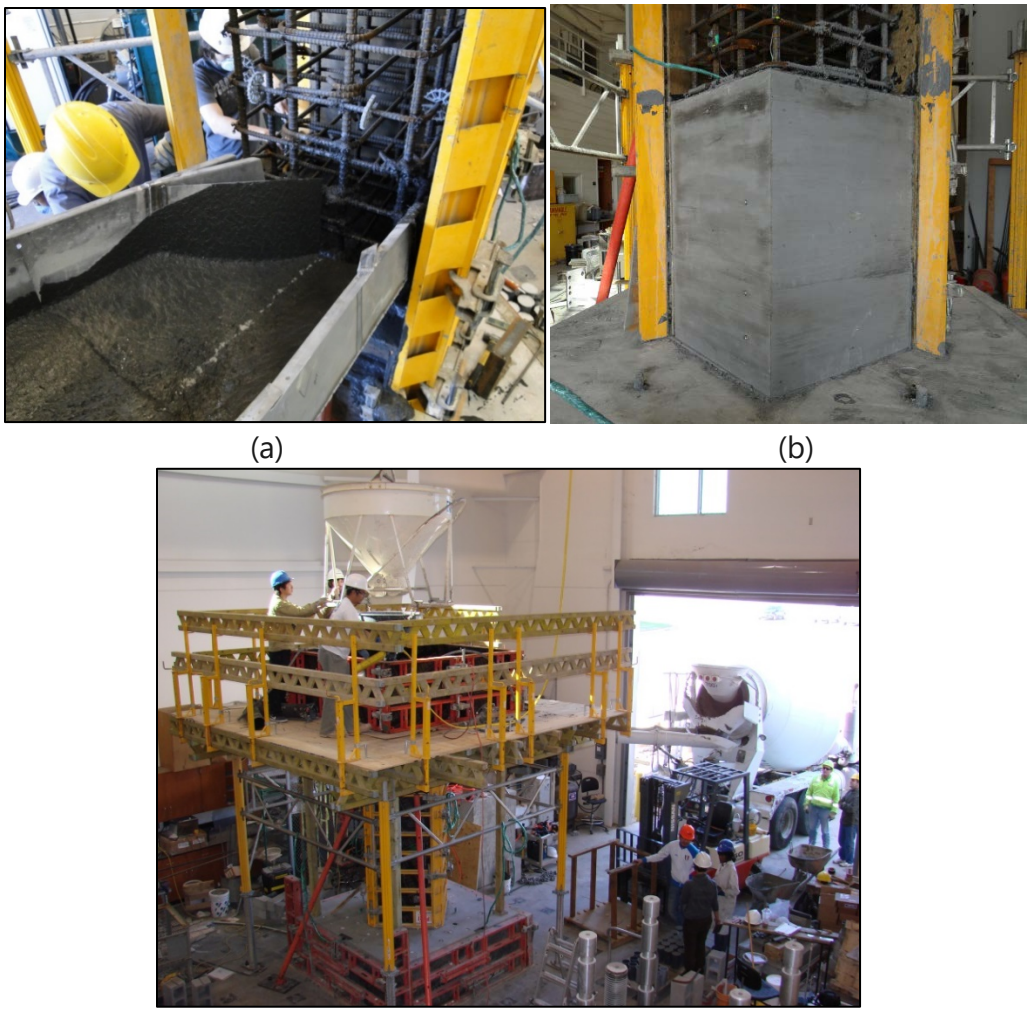

Figure 6. UHP-FRC (a) pouring, (b) completed section, and (c) final casting.

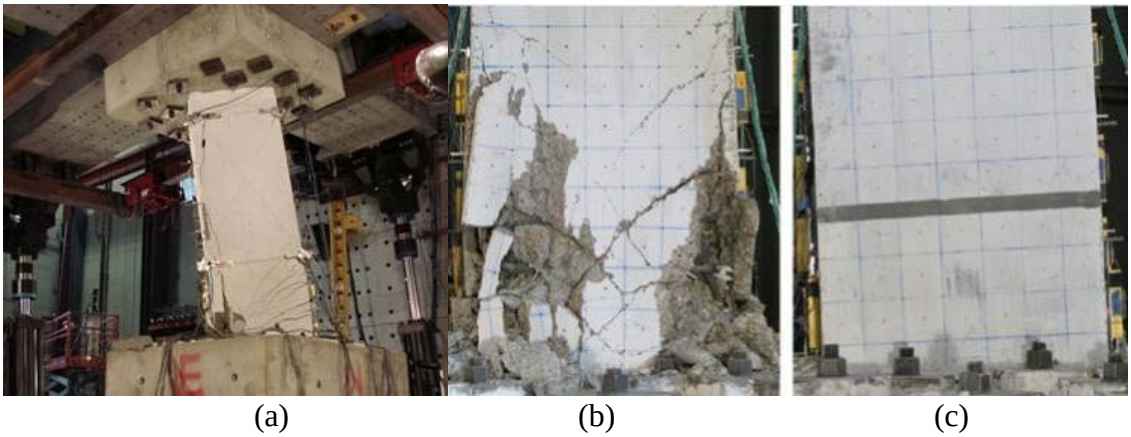

Figure 7. Experimental testing at NSF MAST laboratory (a) Test setup, (b) conventional reinforced concrete column, and (c) UHP-FRC concrete column.

The applications of UHP-FRC in precast products was also explored by the UTA's research team. One of the applications included the concrete sandwich façade panel discussed above. In conventional panels, concrete is reinforced with steel reinforcing bars, and the panel is typically 8 to 12 inches thick. The use of UHP-FRC eliminated all reinforcing bars and the thickness was reduced 50%, which translates into a 50% weight reduction. The load test showed (Figure 8) that the cracking resistance of a UHP-FRC façade panel was three times that of the conventional reinforced concrete façade panel even when there were no reinforcing bars in the UHP-FRC façade panel. This test result was very promising because it exhibited the high cracking resistance and durability of UHP-FRC façade panels with reduced weight, cost in labor, transportation, and installation.

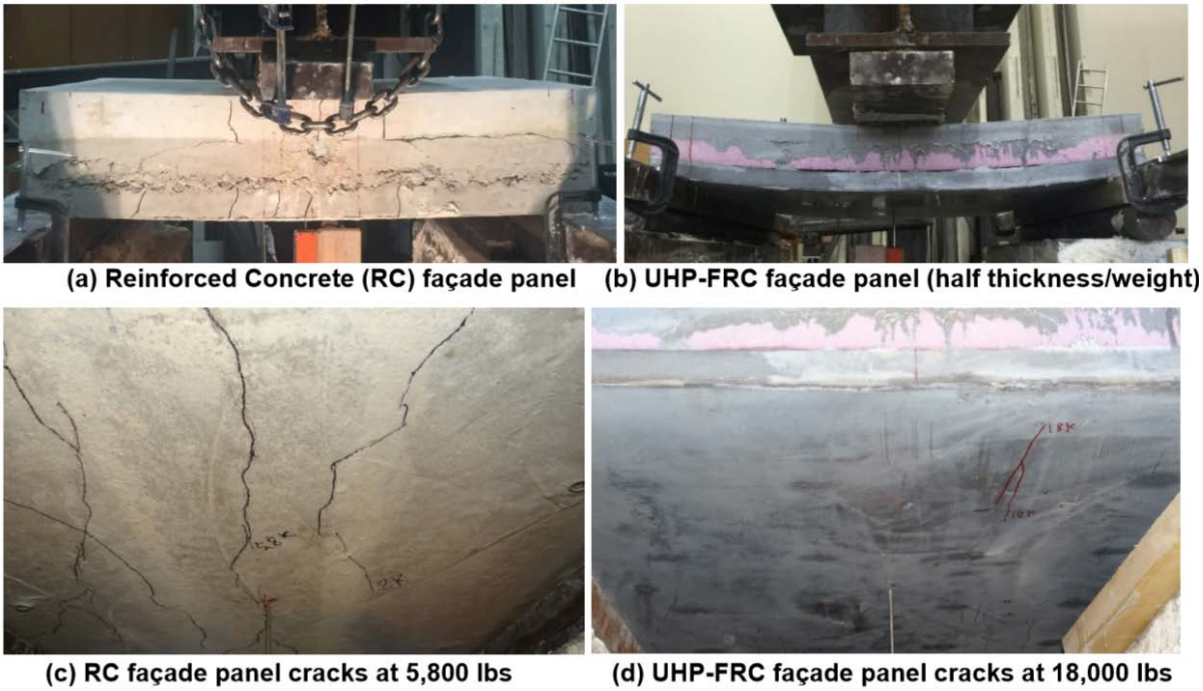

Figure 8. Load testing of RC and UHP-FRC façade panels at UTA CELB.

The advantages of UHP-FRC materials are:

1. High-strength and high durability as compared conventional concrete pavement: the ultrahigh strength and dense microstructure of UHP-FRC allows much thinner and durable pavement and complete removal of conventional reinforcement. The high durability comes from a very dense microstructure due to dense particle packing design and low water ratio used. This leads to a very low permeability (about 1% of conventional concrete) which in turn leads to a very durable concrete material *(15)*.
2. UHP-FRC also serves an excellent option for urgent repair which allows minimal downtime due to its high early strength (one-day strength about 10 ksi) (Figure 5b).
3. UHP-FRC's high damage tolerance capability can significantly reduce the number of joints as well as any pop out of concrete after cracking (Figure 7). UHP-FRC can take much greater compression/tension and its ductility allows it to accommodate large

deformation due to temperature change (Figure 9), which permits the use of jointless pavement.

4. UHP-FRC's high cracking resistance (Figure 8) and high strength allows much sustainable pavement and lower life-cycle costs due to considerably reduced repair needs.

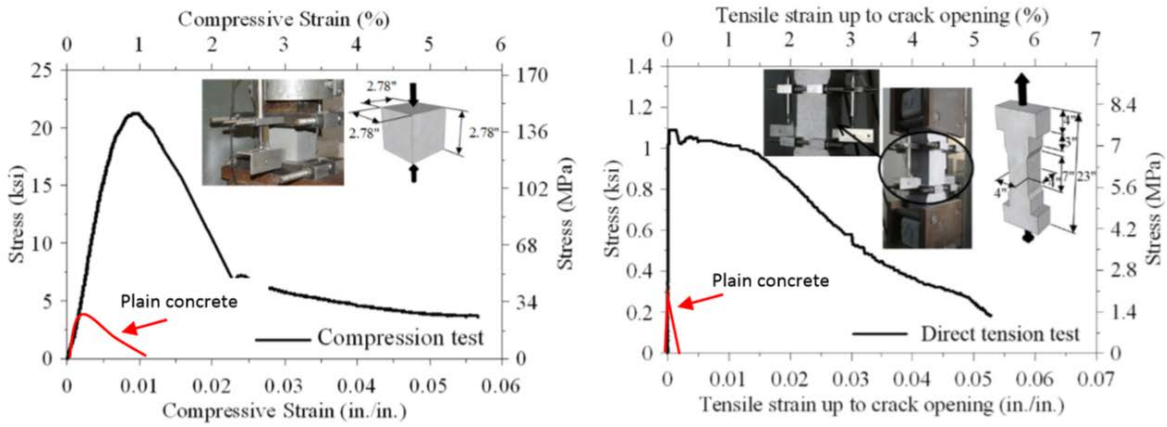

Figure 9. Typical compressive stress-strain of UHP-FRC/plain concrete (left); and direct tension test response for UHP-FRC/plain concrete (right) (17).

While UHP-FRC can significantly enhance the load-carrying capacity and durability of repaired pavement, a sound pavement joint between the existing concrete and UHP-FRC needs to provide adequate transfer of loads. Load transfer can be obtained by using dowel bars or by cohesion/aggregate interlock. A prior research carried out by our research team *(18, 19)* using large-scale push-off test (Figure 10) with various magnitudes of surface roughness (Figure 11) indicated that a rougher surface is able to provide strong interface shear resistance of approximately 0.2 ksi. The results also indicated that dowel bars are effective only when certain slip of the interface occurs. Therefore, the cohesion/aggregate interlock is the primary resistance before slip occurs. Considering the high shear resistance (in the range of 0.2 ksi), it is possible for the joints to provide sufficient strength by using a roughened surface.

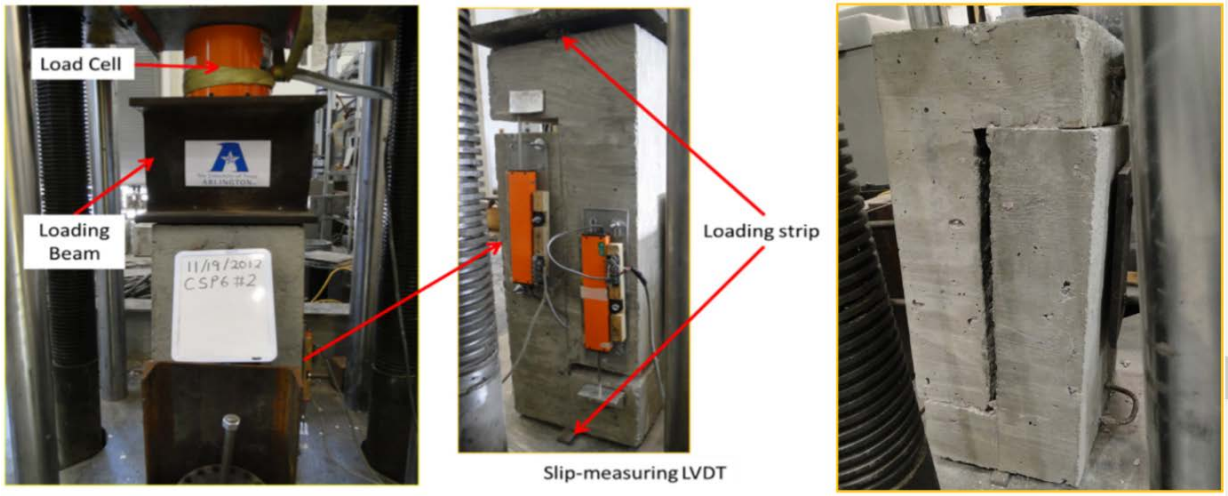

Figure 10. Push-off test setup (18, 19).

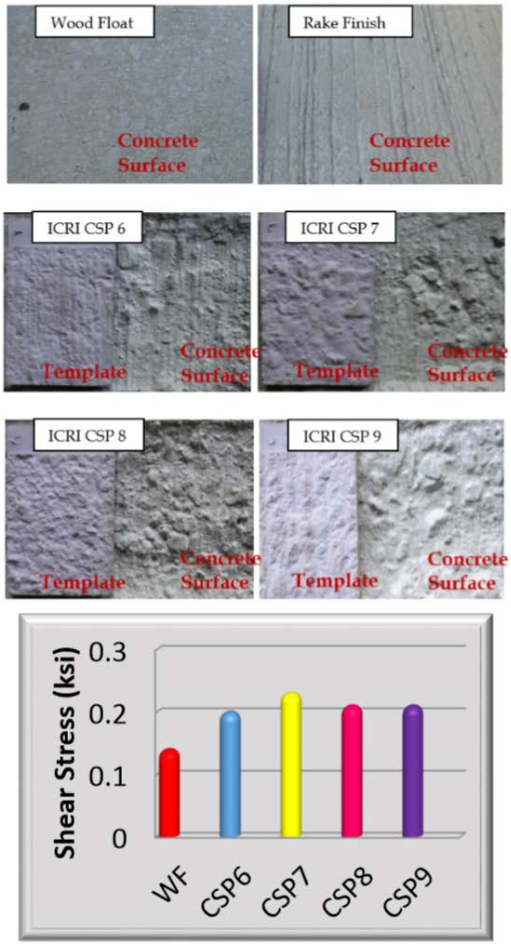

Figure 11. Surface roughness and the corresponding cohesion/aggregate interlock resistance.

1.2.2. UHP-FRC in Repair

Overlay in pavements and bridge decks repair is the majority transportation infrastructure applications of UHP-FRC to UHP-FRC overlay shows greater bond strength between the substrate concrete and the UHP-FRC overlay than that of the substrate concrete. UHP-FRC also exhibits a significant increase in flexural strength and toughness, post cracking tensile capacity, high resistance to environmental and chemical attack, and negligible permeability *(20–23)*.

UHP-FRC has been used in limited pavement and deck repair. UHP-FRC was used successfully in a pilot project for the repair and upgrade of an existing reinforced concrete motorway bridge in a high-level road network in Austria *(24)*. Toppings and deck panels using UHP-FRC were employed in the rehabilitation of the orthotropic bridge deck, in the Netherlands *(25, 26)*. Log Cezsoski Bridge in Slovenia used UHP-FRC in bridge deck overlay *(27)*.

There is almost no literature review regarding the use of UHP-FRC in pavement repair *(28)* similar to the one proposed in this study.

2. OBJECTIVE

The objective of this project focused on utilizing UHP-FRC's high durability, early strength, and ductility for repair of concrete pavements. This was achieved as follows:

- Optimization of the UHP-FRC mix design. This research confirms the UHP-FRC properties as capable of meeting the requirements of pavement placement in terms of flowability, surface preparation and high early strength gain.
- Study of the advantages of using UHP-FRC in pavement repair.
- Evaluation of the existing pavement repair practices and investigation of the possibility of using UHP-FRC for pavement repair without significant change in current practices.
- Development of a simple, time-saving, and sustainable approach to using UHP-FRC for pavement repair.

3. SCOPE

This report explores the possibility of the use of UHP-FRC in the pavement repair. Trials with different mix designs were conducted for the optimum UHP-FRC mix design to be used. The results of the trial mixes are presented in this report.

Experimental tests, slant shear test and punch test, were conducted to evaluate and compare the interface bond strength between existing repair method and the proposed new repair method using UHP-FRC. The results of the tests are presented.

Also, the report includes the results of an LCCA considering the initial material cost, long-term maintenance cost and user costs related to the proposed UHP-FRC pavement repair along with a comparison to the conventional concrete repair method.

4. METHODOLOGY

The primary purpose of this research is to investigate the advantages of using UHP-FRC over conventional concrete in pavement repair. For this, the first part of this research involves trials with different constituents and mix proportions. This research focused on delineating the behavior of UHP-FRC when used as a repair material in the full- and partial-depth repair of pavement. Thus, a proper understanding of the shear transfer across the interface between the old concrete and new UHP-FRC repair material is necessary. In this study, the research team used a slant shear test (SST) and punch test to examine the interface shear strength.

4.1. Trial Mix

In this phase, varying proportions of individual components and different kinds of fibers were tried to obtain the desired compressive strength of UHP-FRC. Steel fibers (Figure 12) have been used in UHP-FRC as they provide great mechanical properties to the concrete mix. However, steel fibers may not be suitable for pavements because of liability issue concerns. In this regard, synthetic fibers (Figure 12) can serve as a better alternative. The mechanical properties of the fibers used are shown in Table 3.

Figure 12. Micro steel fiber (left) and ultra-high molecular weight polyethylene fiber (right).

Table 3. Mechanical properties of the fibers used.

Fiber	Length (mm)	Diameter (mm)	Tensile strength (ksi)
Micro steel fiber	13	0.12	313
UHMW Polyethylene fiber	13	0.0015	375

4.2. Slant Shear Test (SST)

SST is an ASTM standard testing method *(29)* and adequate to predict the strength of concrete-to-concrete interfaces in shear. However, while ASTM C882 requires the SST specimen be made of two equal sections of a 75×150-mm [3×6-in.] cylinder, each section had a diagonally cast bonding area at a 30° angle from the vertical position. Extensive numerical finite element simulations carried out by Santos *(30)*, suggested a prismatic SST specimen with a 150×150×560 mm^3 [5.9×5.9×22 in^3] with a shear plane at a 30-degree angle from the vertical position (Figure 13). The optimal geometry for SST specimens was determined based on: a) obtaining an acceptable stress distribution along the interface, b) adopting a single geometry for all slant shear specimens, only varying the shear plane angle and the corresponding total height *(30)*. The following geometry with a cross section of 150×150 mm^2 [5.9×5.9 in^2] will be used in this research. Different concrete surface profiles (CSP) as defined by the International Concrete Repair Institute (ICRI) were used. CSP are numbered from 1 to 9 in with the surface CSP9 being the roughest and CSP1 the least rough.

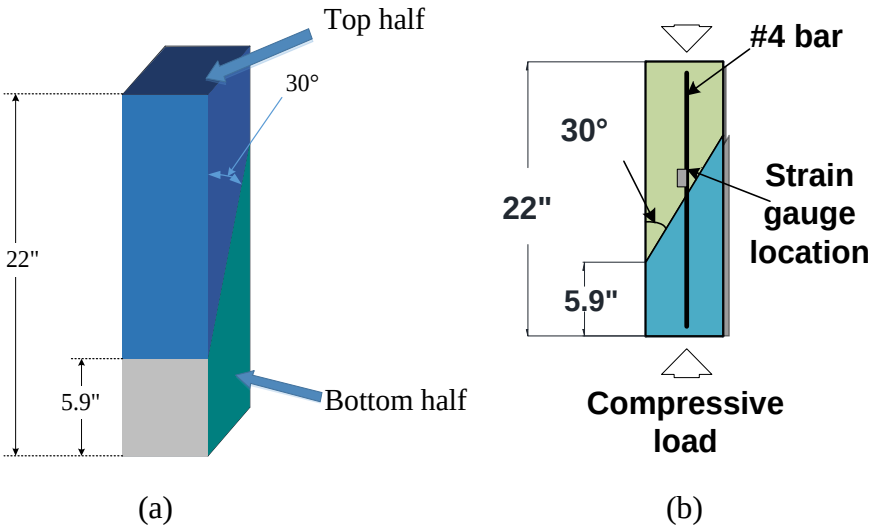

Figure 13. (a) Slant shear test specimen and (b) slant shear specimen showing rebar and strain gauge location.

4.2.1. Specimen Preparation

Three types of specimens were prepared. In the first type, the inclined surface of the bottom half was cut smooth. Then, vertical holes were drilled parallel to the long face of the specimen.

1. A wood support (Figure 14) was prepared to provide an incline casting surface at an angle of 30°. The mold was placed on the support with its back face resting on the inclined support as shown below. Then, the bottom half of the mold was cast, covered by plastic sheeting and cured at normal room temperature for a minimum of six days.

Figure 14. Mold placement and casting for bottom half of slant shear specimen.

2. The specimen was demolded and the inclined surface was cut to a smooth surface using a concrete saw (Figure 15a). This step is necessary to simulate the actual saw cutting in the field repair. This cutting results in a smooth surface of the inclined plane (Figure 15b).

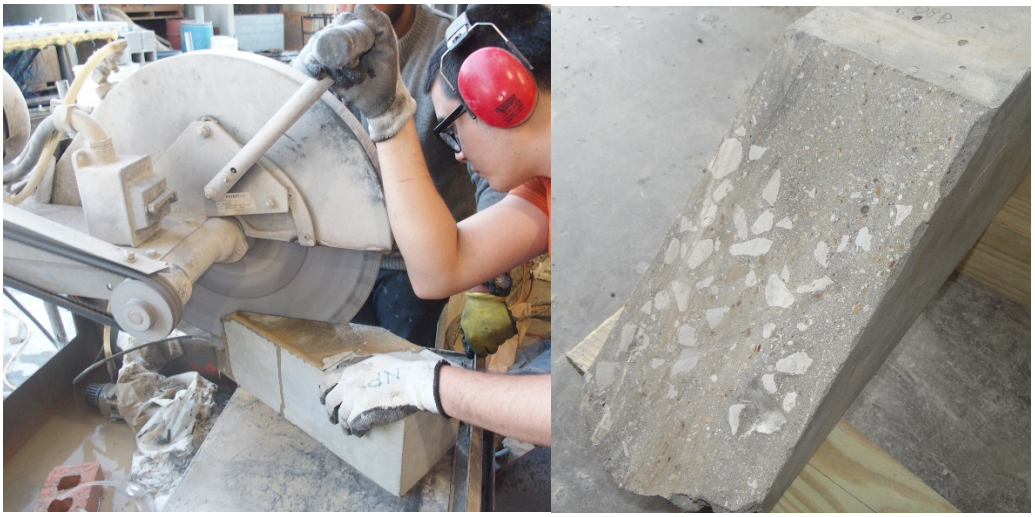

(a) (b)

Figure 15. (a) Using concrete saw to smooth cut the incline surface and (b) smooth cut surface after sawing.

3. The next step is to treat the inclined surface of the bottom half as per specimen requirement for the top half. Based on the type of specimen to be prepared, the following steps should take place.
    a. To prepare a specimen with a smooth surface and an embedded reinforcement bar:
        i. First, vertical holes were drilled parallel to the long face of the bottom half (Figure 16a, 16b) to a depth of 8 inches. Then the holes were cleaned of dust. For this, a blow-out gun (Figure 16c) is used to blow-out the hole twice followed by brushing out the hole twice. Then the hole is blown out two more times. This ensures that maximum bonding can be obtained while anchoring the rebar.

(a) (b)

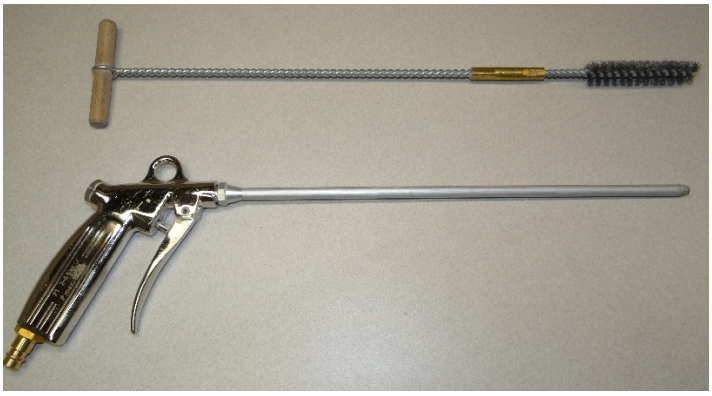

(c)

Figure 16. (a) Drilling of holes in bottom half, (b) finished holes in two specimen bottom halves, and (c) manual brush and blow-out air pump used for specimen preparation.

ii. Then, epoxy is inserted in the drilled hole and a rebar is embedded into the drilled hole with a slight twisting motion. Once the epoxy is set, the strain gauge is installed on the rebar one inch away from the interface as shown in Figure 17.

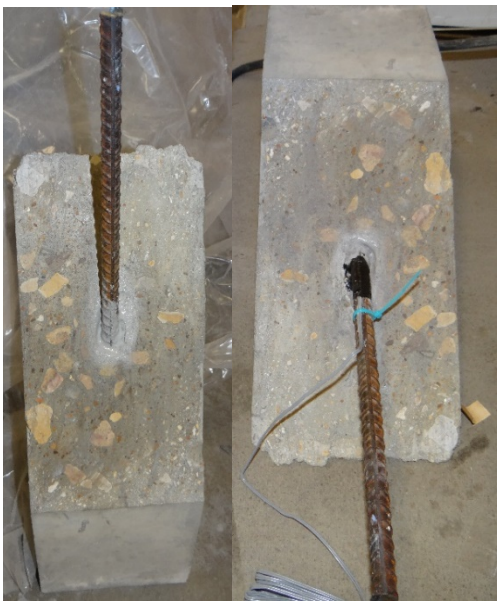

(a) (b)

Figure 17. (a) No. 4 rebar anchored in bottom half and (b) strain gauge installed in rebar.

b. To prepare the specimen with the roughened surface, the surface was roughened using a pneumatic needle scaler (Figure 18a) to desired concrete surface preparation level as shown in Figure 18.

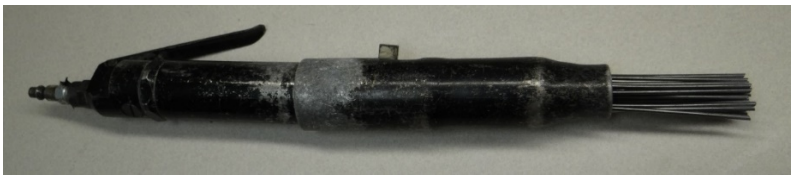

(a)

(b) (c)

Figure 18. (a) Pneumatic needle scaler used for surface roughening. The saw cut inclined surface (b) before and (c) after roughening.

c. For the specimen with the smooth surface without any embedded rebar, the saw cut surface is left as it is.

4. The prepared specimen is then positioned in the mold in the orientation shown in Figure 19; then, the top half of the material is cast, after which the specimen is covered with plastic sheeting and cured at room temperature.
5. The specimen is then demolded and tested.

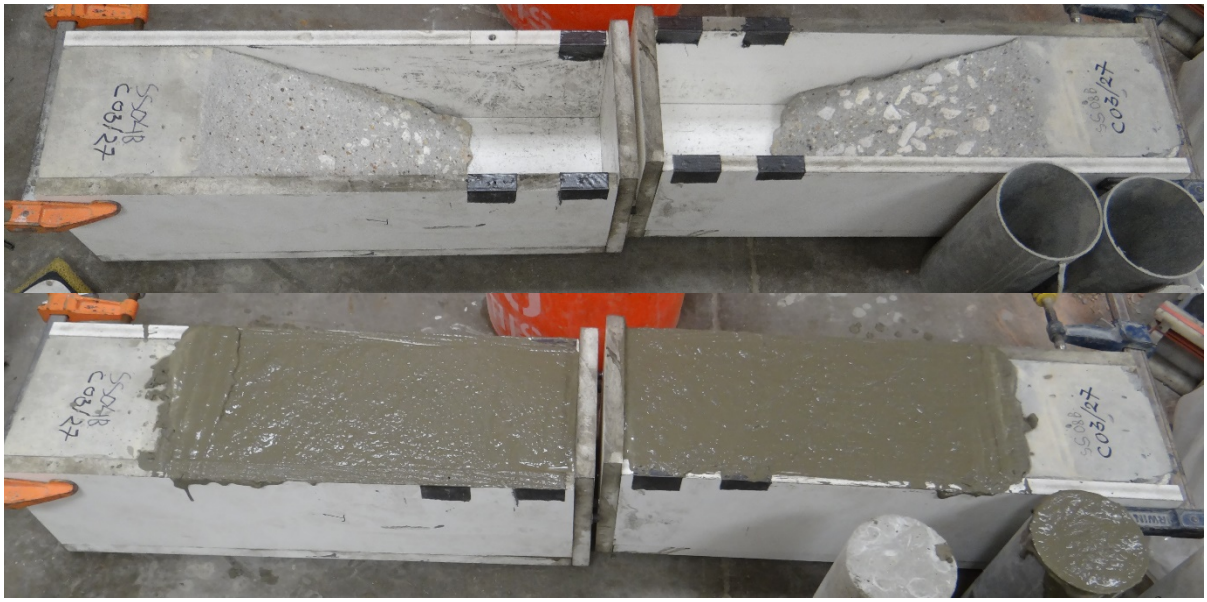

Figure 19. Casting of top half of the slant shear specimen with PC with roughened surface (CSP 7).

4.2.2. Testing

A specimen was prepared in two stages. The bottom half represents the existing concrete of the pavement and the concrete in the upper half represents the new repair pavement concrete. Molds and support were fabricated to allow the preparation of such a specimen. The bottom concrete was cast using the concrete mix of 1:1:2 with a water-to-cement ratio of 0.5. Curing was performed under ambient temperature, and the cast concrete was covered with plastic sheets. The cylinder tests of the concrete mix provided a 6-day compressive strength of 2960 psi. The bottom half was left to cure for a minimum of 6 days before additional casting was done on top of it. The top half was cast for different concrete mixes and tested in one day. Tests were done using a loading rate of 0.02 in/min. Displacement control was chosen over load control to incorporate the post-peak data for the slant shear tests for the specimens with a rebar embedded on it. The same displacement control loading was adopted for other slant shear specimens to maintain uniformity for all the specimens. Tests were done in a Tinius Olsen SuperL universal testing machine located in the Civil Engineering Laboratory Building (CELB) at UTA. Depending on the top half of the slant shear specimen, the test setup consists of a load cell, a strain gauge and two linear variable differential transformers (LVDTs).

The LVDT was used to measure the vertical deformation and the load cell was used to measure the applied vertical load. The strain gauge (when used) was placed 1 inch above the interface which gave the value of the strain in the reinforcement bar. All sensors were connected to the DAQ box and the data was recorded. The test setup is shown in Figure 20.

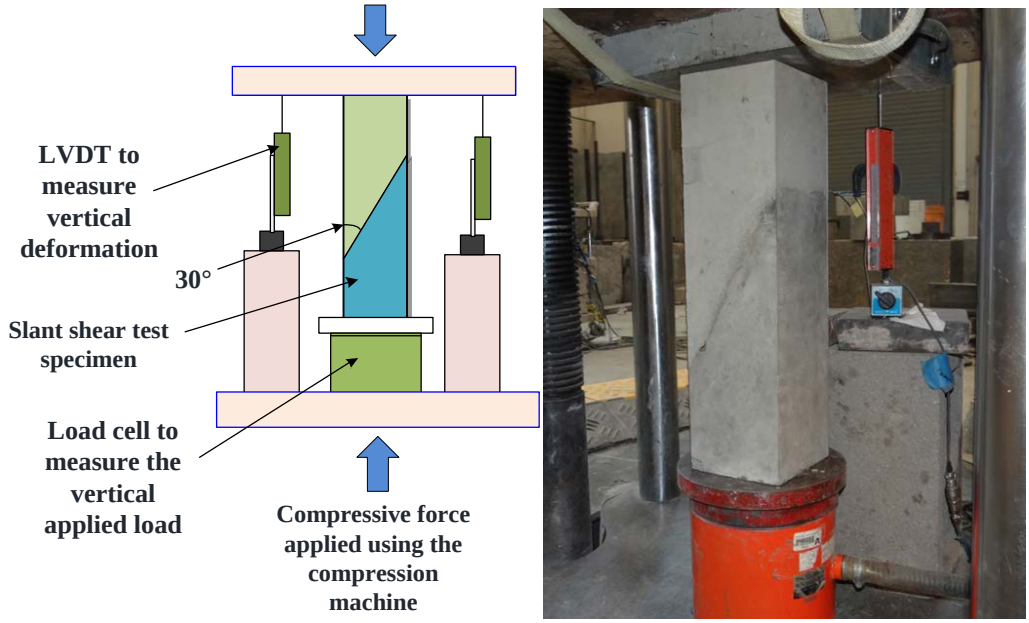

Figure 20. Slant shear test setup.

The shear stress was obtained from the recorded peak's longitudinal load using the formulae presented below:

$$V = P\,cos30° \quad [1]$$

where:
V = Shear force, and
P = Vertical applied load.

$$s = d/cos30° \quad [2]$$

where:
s = Deformation along slip, and
d = Vertical deformation.

$$\tau = V/A_{inclined} \quad [3]$$

where:
τ = Shear stress, and
$A_{inclined}$ = Inclined area.

The following formula was used to calculate the rebar force:

$$A_{eff} = A_{rebar} \times sin30° \quad [4]$$

where:
A_{eff} = Effective area of rebar = 0.2 in^2, and
A_{rebar} = Area of No. 4 rebar = 0.2 in^2.

$$T = \varepsilon \times E_{rebar} \times A_{eff} \quad [5]$$

where:
T = Rebar force,
E = Strain in rebar, and
E_{rebar} = Modulus of elasticity of rebar = 29000 ksi.

4.3. Punch Test

4.3.1. Necessity of Punch Test

The vertical force applied in the slant shear specimen can be divided into two components, the shear force component (P cos30°) acting parallel to the inclined interface and the normal component (P sin30°) acting normal to the inclined surface as shown in Figure 21. The normal component (P sin30°) generates a frictional force (μ P sin30°) which provides additional resistance. This along with the shear strength of the interface provides a combined resistance which causes the overestimation of the shear capacity of the interface.

$$V_n = cA_{cv} + \mu P_n \quad [6]$$

where:
V_n = Shear capacity of the interface,
CA_{cv} = cohesion and/or aggregate interlock which is a function of the surface properties, and
μP_n = friction component resulted due to the normal component of the applied vertical load.

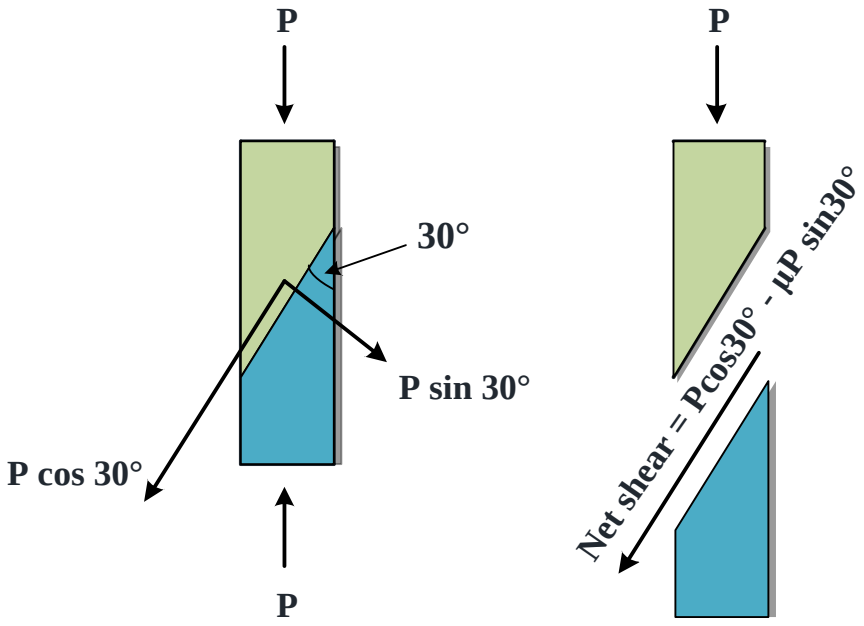

Figure 21. Forces transfer in a slant shear test specimen.

Therefore, a punch test was necessary in this project.

4.3.2. Punch Test Specimen

The punch test for conventional concrete was designed on the basis of the actual repair practices used in the field (Figure 22).

Figure 22. Conventional concrete repair.

A new method for concrete repair was proposed combining the features of precast UHP-FRC with cast-in-place repair of pavement without any dowel bars (Figure 23). In this method, a precast UHP-FRC panel is used along with cast-in-place UHP-FRC. The vertical repair surfaces of the existing concrete are roughened on site. The outer edges of the UHP-FRC precast slabs are roughened before brought to the site (no dowel bars are needed). The depth of the precast UHP-FRC is same as the existing pavement slab thickness. Only a small cast-in-place UHP-FRC joint (one to two inches wide) is done onsite. The roughened precast UHP-FRC slab is placed in the repair area and UHP-FRC is cast in the joint. Note that a prior case study for airfield pavement indicated that a 6,000-ft taxiway reconstruction was done by using precast panels with only overnight closures, compared with a 90-day closure for conventional methods *(31)*.

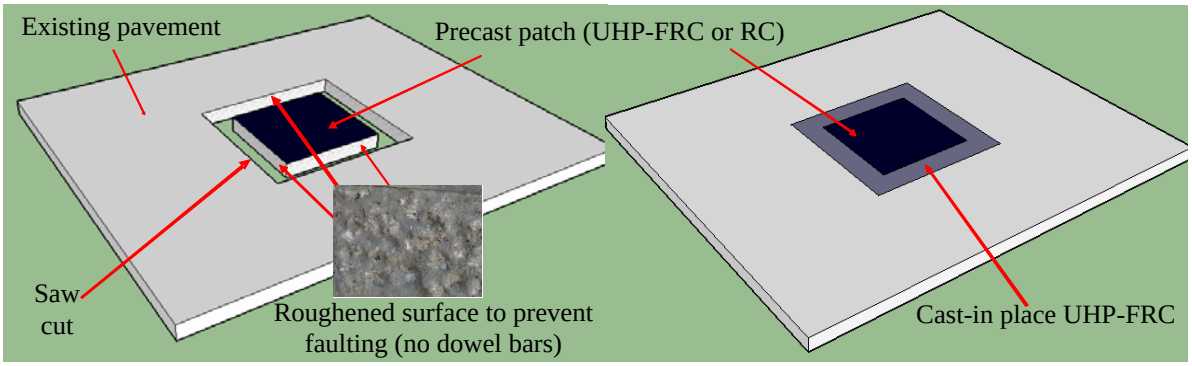

Figure 23. Proposed method for UHP-FRC pavement repair.

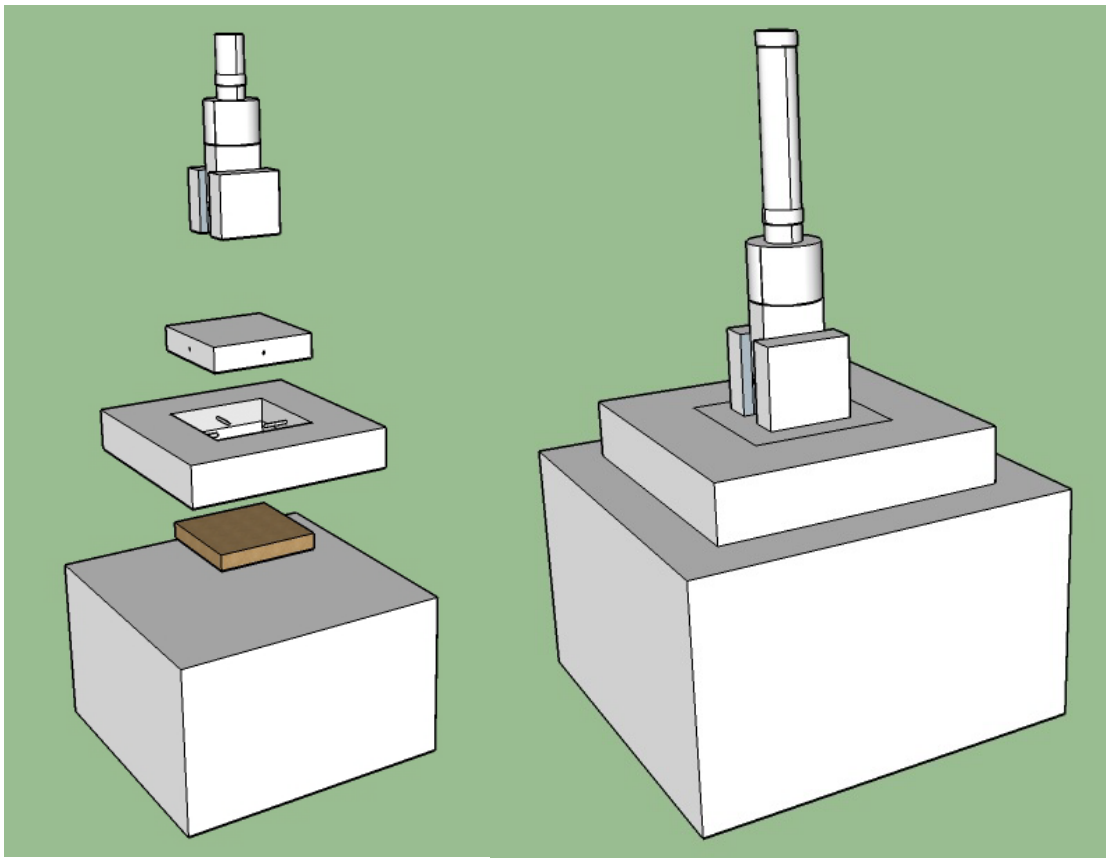

(a) (b)

Figure 24. Punch test setup (a) exploded view and (b) normal view.

The proposed idea was verified by the punch test shown in Figure 24. Two punch specimens were designed to compare the interface shear capacity between the existing concrete pavement and the repair concrete material. Both specimens consist of an outer hollow slab with external dimensions of 50 × 28 in^2 [1270 × 711 mm^2] and internal hollow section with dimensions of 30 ×10 in^2 [762 × 254 mm^2] with a total depth of 10 inches [254 mm]. The depth of the inner repair slab for both the specimens was selected as 4 inches [101 mm].

The first specimen was prepared to simulate the actual repair methods used in practice. Four No. 4 rebars of 17 inches were used as dowel bars with 8.5 inches embedded in the outer hollow slab and remaining in the inner cast-in place slab as shown in Figure 25. The rebars were positioned at a depth of 2 inches from the top surface (mid depth of the repair cast in place concrete slab). Strain gauges were placed in each dowel bar one inch from the interface.

For the second specimen, UHP-FRC was used. A precast UHP-FRC slab with dimensions of 26 × 6 × 4 in^3 was placed in the middle of the repair area and the remaining area was filled with cast-in-place UHP-FRC (Figure 26). The primary purpose of using the UHP-FRC precast panel is to significantly reduce the required volume of UHP-FRC to be cast on site. This would make it more convenient and further aid in reducing the curing time of the cast-in-place UHP-FRC pavement repair.

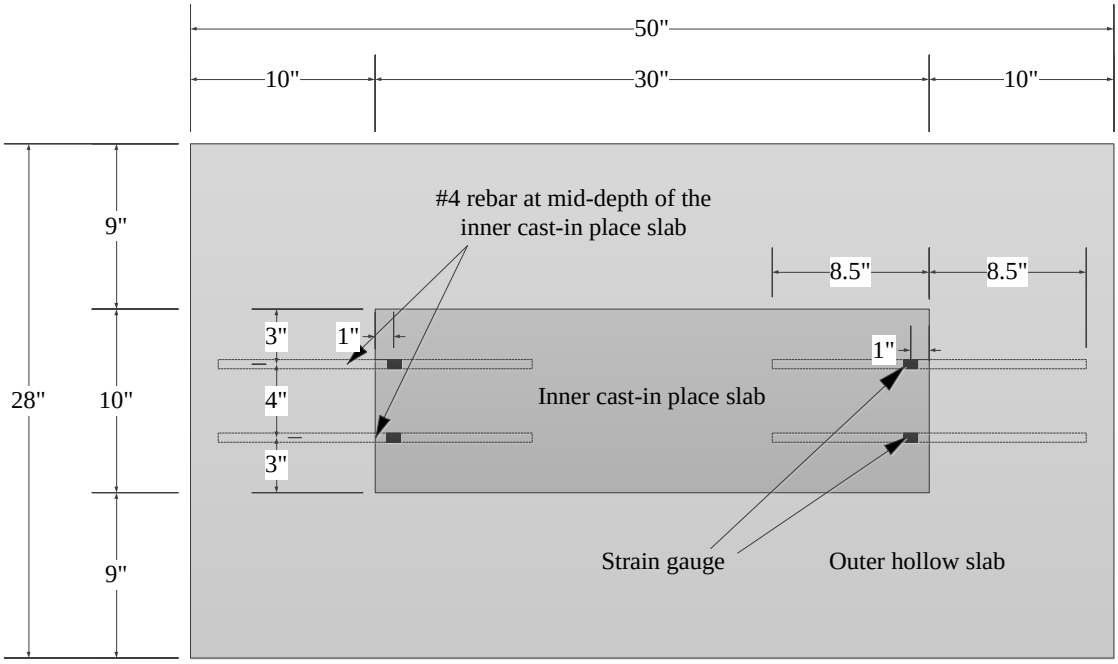

Figure 25. Specimen details for punch test specimen with No. 4 rebars and cast-in-place PC.

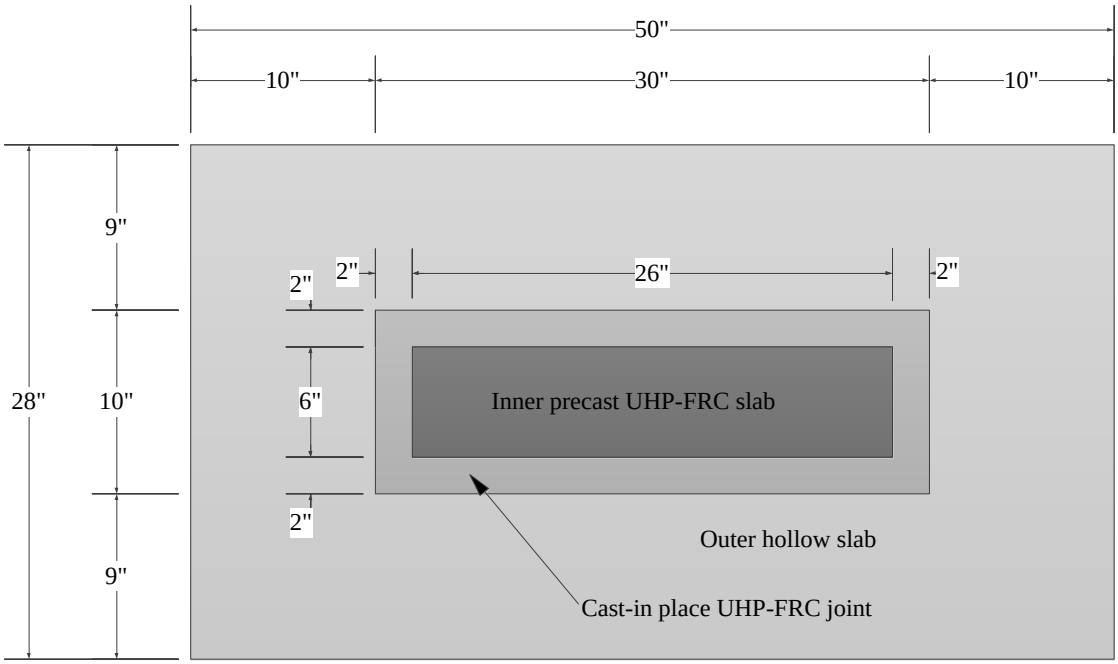

Figure 26. Specimen details for punch test specimen with an inner precast UHP-FRC slab and a cast-in-place UHP-FRC joint.

The preparation of formwork, mixing, and casting of the outer hollow slab is presented below from Figures 27 to 28. The concrete surface after the removal of the specimen from the formwork is shown in Figure 29.

Figure 27. Formwork for the outer hollow slab.

Figure 28. In-lab concrete mixing is shown in top photo and casting for the outer hollow slab is shown in the bottom photo.

Figure 29. Concrete surface roughness (cast in contact with wood formwork).

4.3.3. Punch Test Specimen Preparation

Preparation of punch specimen with dowel bars and cast-in-place PC:

1. Holes 8.5 inches deep (shown in Figure 30) were drilled in the outer hollow slab at a depth of 2 inches from the top surface. Then the hole was blown out twice, brushed out twice, and blown out twice again. Epoxy was then put in the hole and a rebar was inserted with a slight twisting motion. Figure 31 shows the specimen after the insertion of rebar.

(a) (b)

Figure 30. (a) Drilling in the outer hollow slab for rebar placement and (b) rebar length inside the newly repaired concrete.

Figure 31. Outer hollow slab showing embedded rebar location.

2. Then, the strain gauges were installed one inch from the interface as shown in Figure 32.

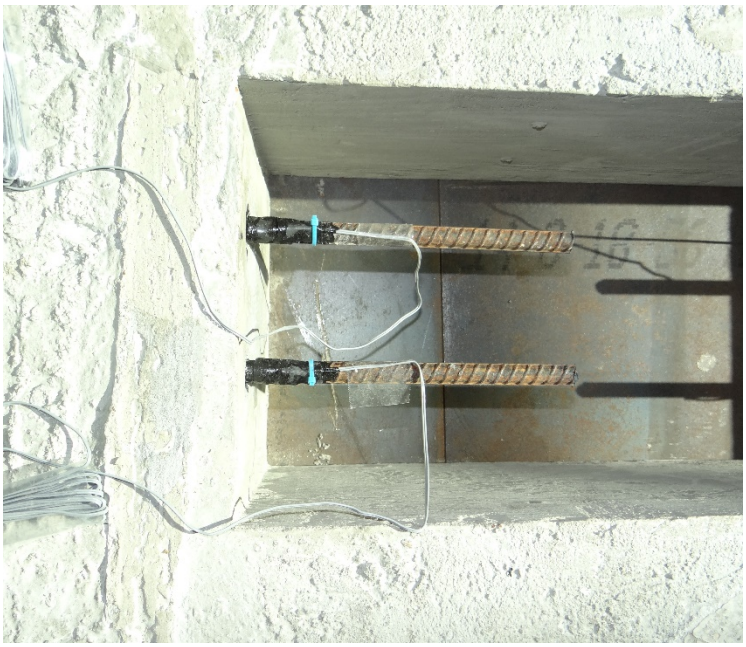

Figure 32. Strain gauges installed on the rebar 1 inch from the interface.

3. The outer hollow slab with the rebar installed with the strain gauge was setup on the compression machine on a steel support.
4. The hollow portion was filled with 6 inches of sand and slightly compacted to provide a firm base for casting 4 inches of cast-in-place plain concrete as shown in Figure 33.

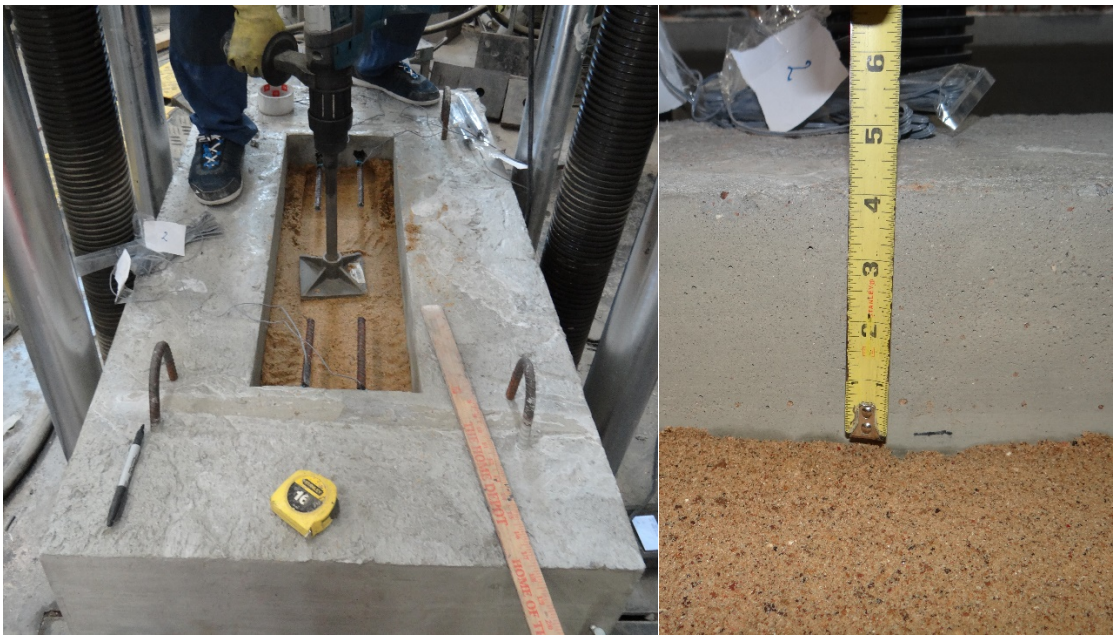

Figure 33. Placing and compacting the sand in the hollow portion of the slab to provide a firm support for casting 4 inches of cast-in-place PC.

5. Finally, PC is cast in place on the sand (Figure 34).

Figure 34. Cast in place PC punch test specimen.

Preparation of punch specimen with UHP-FRC:

1. First, the precast UHP-FRC precast panel was cast (Figure 35). After casting, the concrete was heated using heaters to provide an average temperature of 100°F.

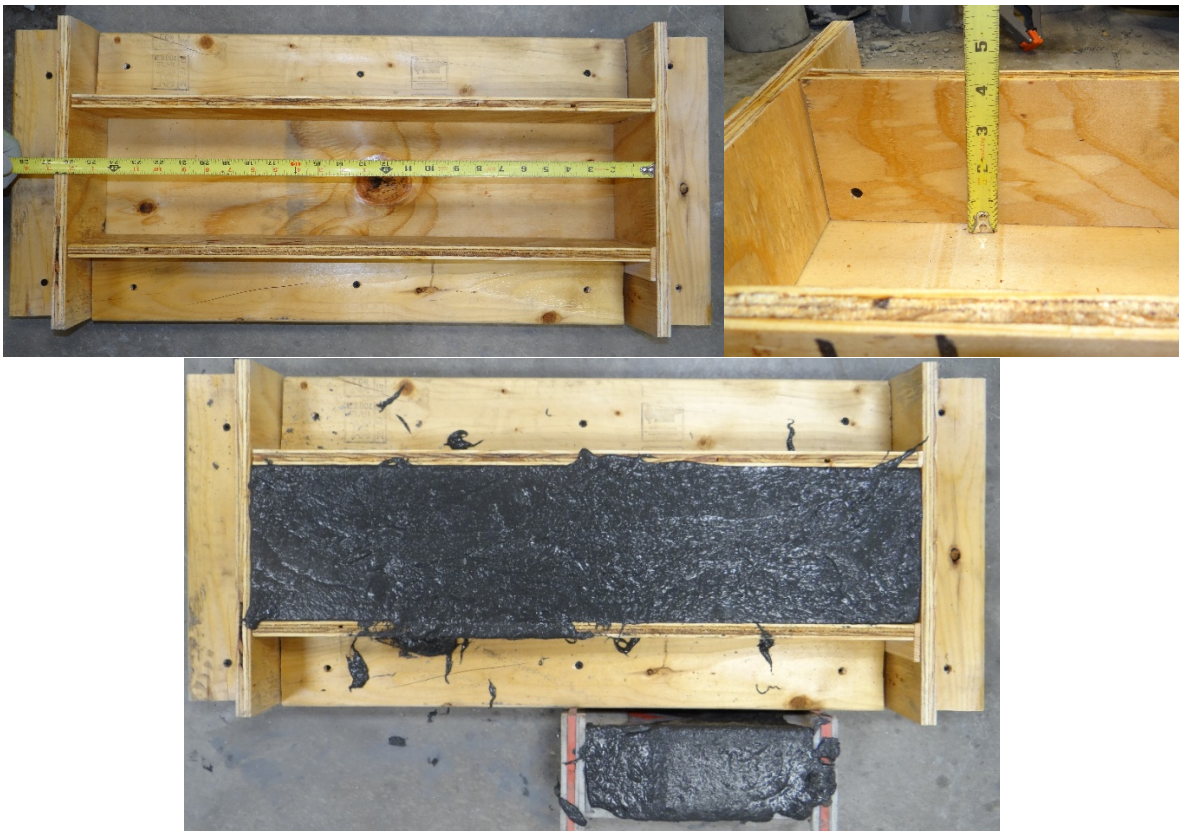

Figure 35. Formwork and casting of the UHP-FRC precast panel.

2. Then, the inner surface of the hollow slab was roughened to a depth of 4 inches from the top. A pneumatic needle scaler was used to get a CSP 5 roughness level (Figure 36).

Figure 36. Roughened surface of inner wall of the outer hollow slab with a depth of 4 inches with a roughness level of CSP 5.

3. After that, the outer slab was placed on steel supports in the compression machine. Sand was filled and compacted in the bottom 6 inches of the hollow portion, which provided a depth of 4 inches from the top for placement of the UHP-FRC precast panel and UHP-FRC casting (Figure 37).

Figure 37. The 4-inch casting surface level obtained after placement and compaction of sand in the hollow portion.

4. The UHP-FRC precast panel was placed in the center of the hollow part as shown in Figure 38 and UHP-FRC was cast in place in the joint between the precast UHP-FRC panel and the outer hollow slab (Figure 39).

Figure 38. Placement of precast UHP-FRC panel into hollow portion of outer hollow slab.

Figure 39. Cast in place UHP-FRC between the precast UHP-FRC slab and outer hollow slab.

5. Finally, the cast in place UHP-FRC is heated using a combination of lamps to obtain an average temperature of 100 °F (Figure 40).

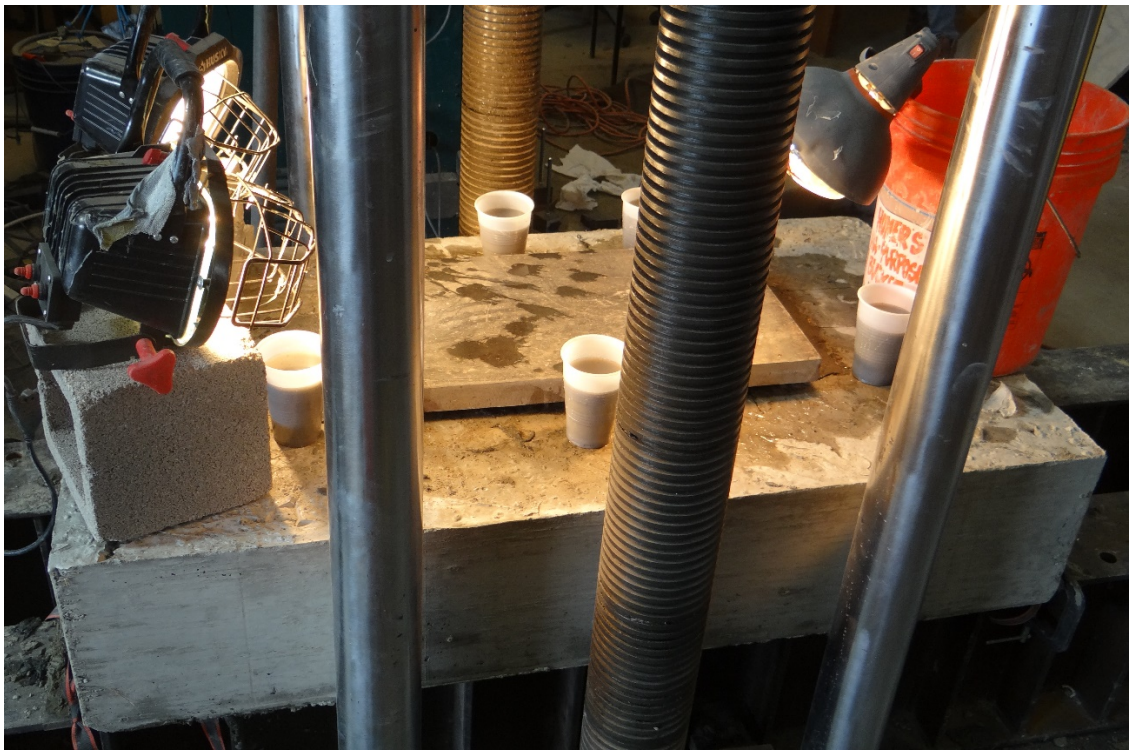

Figure 40. The cast-in-place UHP-FRC repair joint heated to an average temperature of 100 °F using a combination of heaters.

4.3.4. Testing

The specimen was tested one day after casting of the hollow portion of the outer hollow slab (PC and UHP-FRC). The tests were done using Tinius Olsen SuperL universal testing machine located in the Civil Engineering Laboratory Building (CELB) at UTA. Tests were done using a loading rate of 0.02 in./min. Displacement control was chosen over load control to incorporate the post-peak data for the punch specimens. Similar to the slant shear test, LVDT was used to measure the vertical deformation and a load cell was used to measure the applied vertical load. The strain gauge (when used) was placed one inch above the interface, which gave the value of strain in the reinforcement bar. All the sensors were connected to the DAQ box and the data was recorded. Uniform loading was applied in the central 18 × 9 in^2 area using two 9 × 9 × 2 in^3 square steel plates. A 0.5-in.-thicksteel plate was placed on top of these two steel plates[2] to keep the plates stationary throughout the loading to assure uniform application. The test setup is shown below in Figure 41.

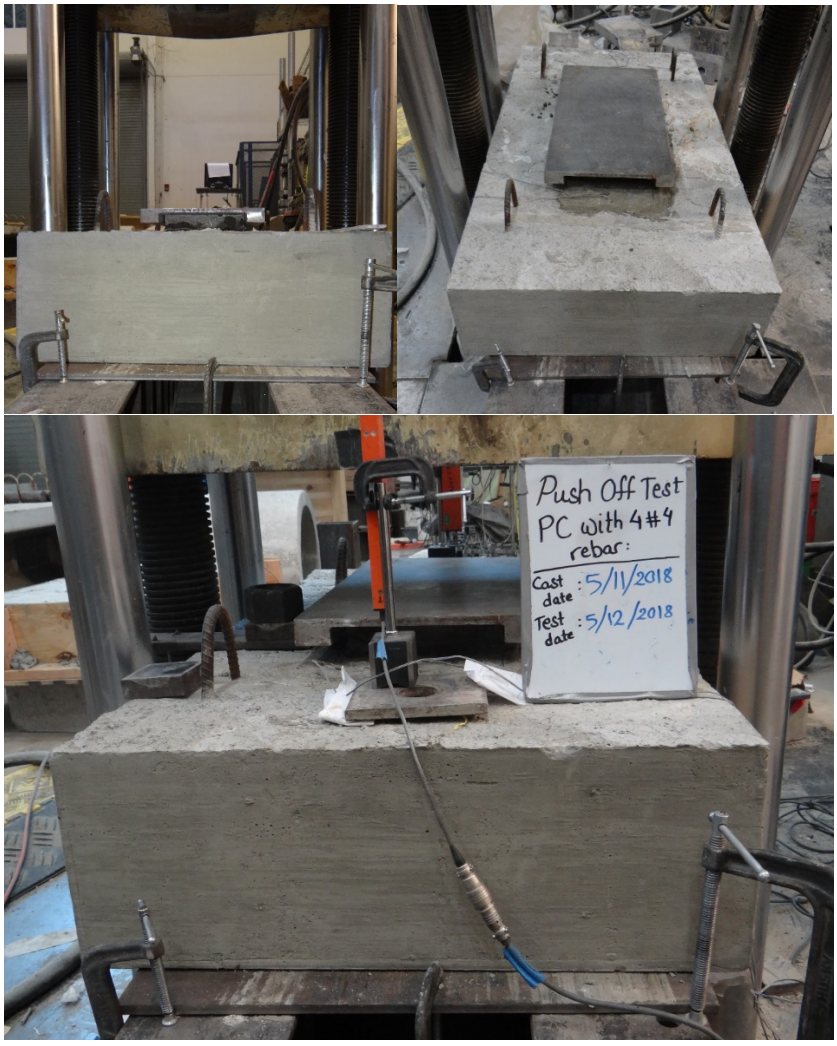

Figure 41. Test setup for the punch test.

5. FINDINGS

5.1. Trial Mix

The results of the trial mix are presented in Table 4. Figures 42–53 show the stress vs. strain graphs of the trial specimens in Table 4.

Table 4. Trial mix design.

Trial Mix	Description	Peak Load			Average Peak Load	Average Compressive Strength	Age of Concrete
		Sample 1	Sample 2	Sample 3			
		kips	kips	kips	kips	ksi	days
1	CL Mix 0.75% LFB: Long polyethylene fiber (LFB)	137.4	148.5	132.7	139.6	18.06	28
2	No GP, 20% Imerfill, Long PE: Glass powder (GP) Polyethylene fiber (PE)	119.2	124.9	125.5	123.2	15.94	28
3	No GP, Long PE	137.8	130.5	133.2	133.8	17.32	28
4	30% FA, LPE 0.75%: Fly ash (FA)	125.6	136.8	119.3	127.3	16.47	14
5	30% FA, LPE 0.1%, SPE 0.65%: Long Polyethylene fiber (LPE) Short Polyethylene fiber (SPE)	114.2	119.8	119.4	117.8	15.24	14
6	30% FA, LPE 0.1%, SPE 0.65%	120.5	115.0	128.7	121.4	15.71	28
7	30% FA, LPE 0.25%, SPE 0.5%	120.0	115.5	-	117.8	15.24	14
8	30% FA, LPE 0.25%, SPE 0.5%	132.1	118.2	-	125.2	16.19	28
9	30% FA, LPE 0.25%, SPE 0.5%(greased)	87.8	-	-	87.8	11.36	14
10	30% FA, LPE 0.75%	121.1	154.4	129.5	135.0	17.47	28
11	3% Steel (greased)	133.1	-	-	133.1	17.22	17
12	20% FA, PE 0.75%	120.4	126.2	115.0	120.6	15.6	14
13	20% FA, PE 0.75%: 150°F	67.4	76.0	84.6	76.0	9.84	1
14	20% FA, PE 0.75%: 100°F	51.8	55.2	52.9	53.3	6.90	1

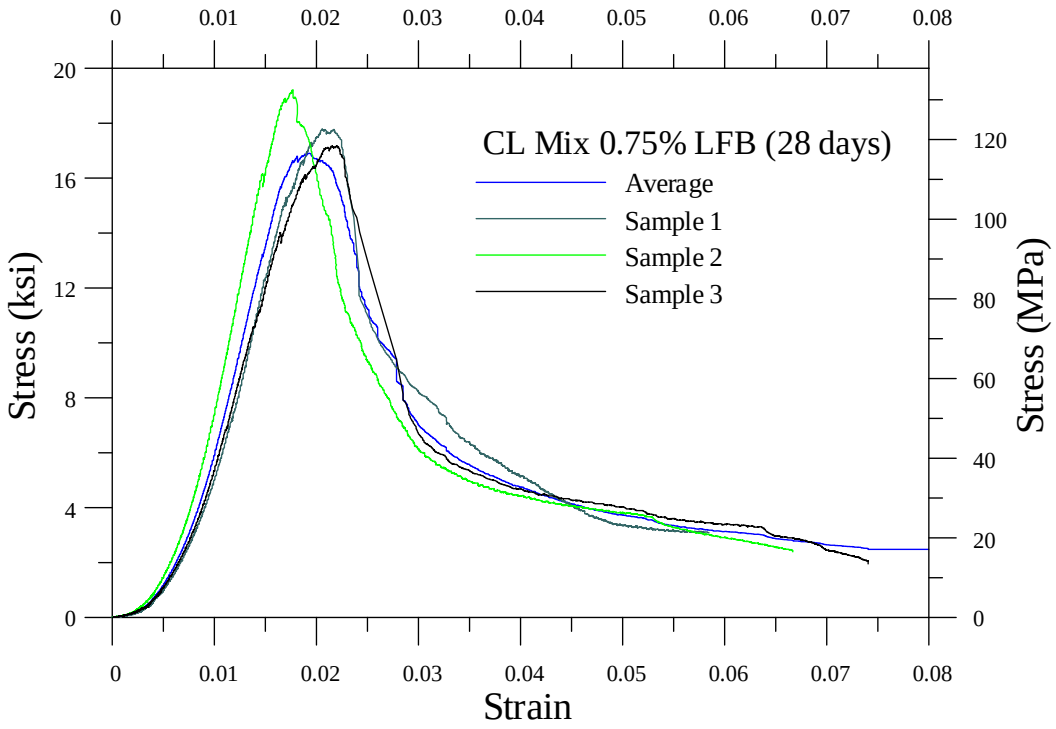

Figure 42. Stress vs. strain (Trial Mix 1: CL mix 0.75% LFB for 28 days).

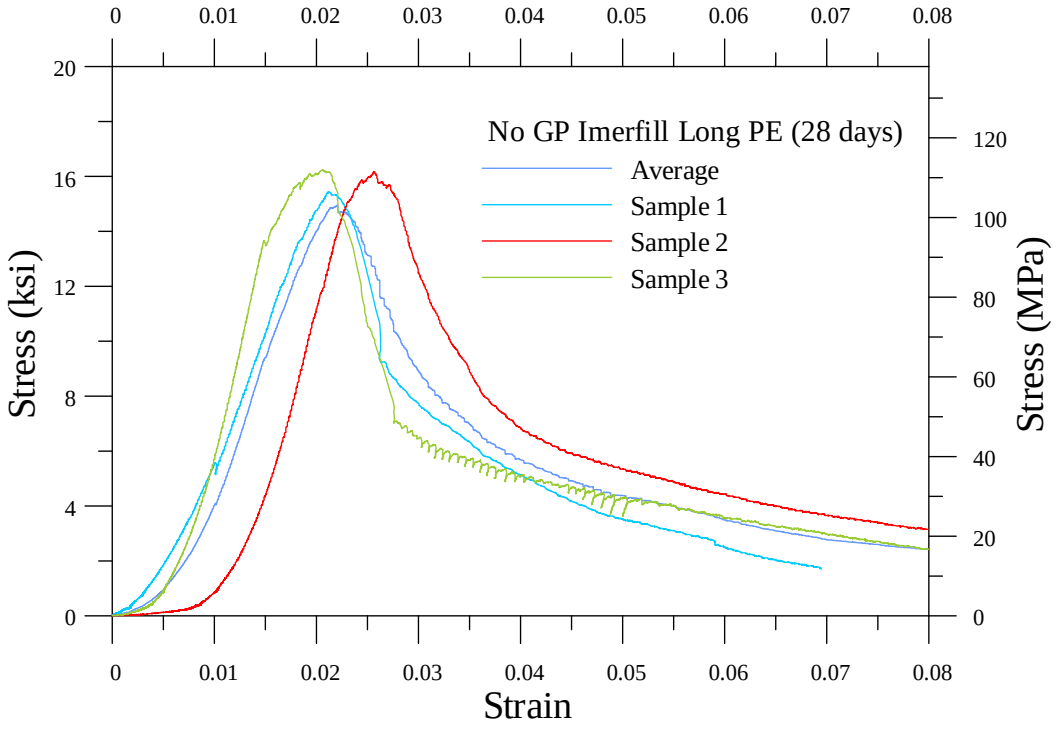

Figure 43. Stress vs. strain (Trial Mix 2: No GP, Imerfill, long PE for 28 days).

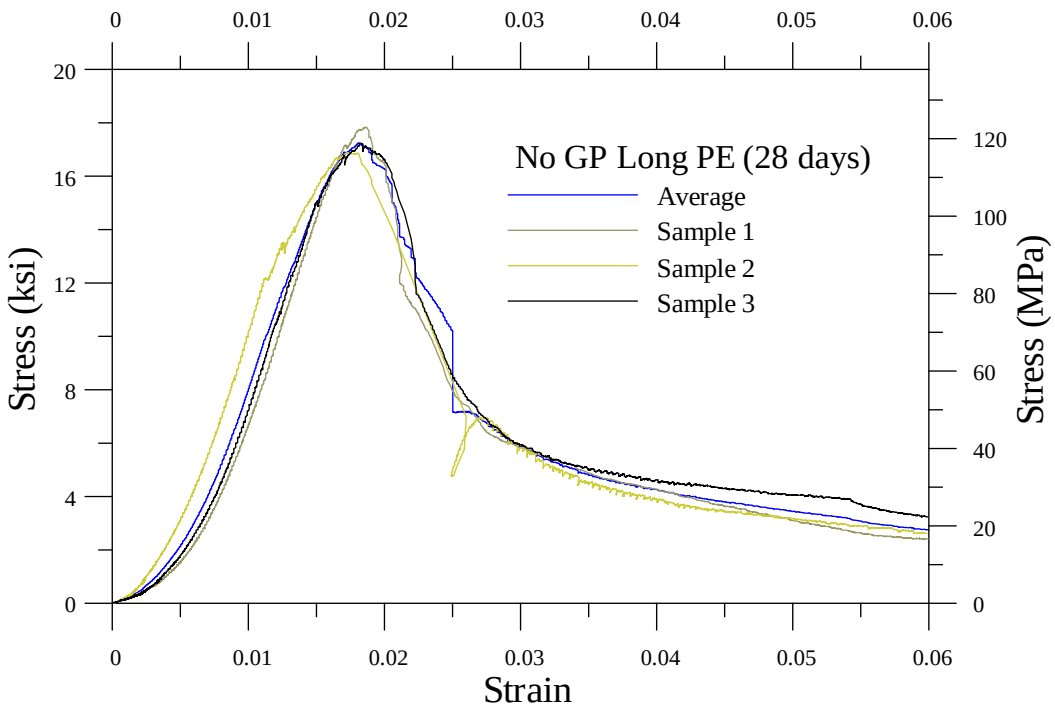

Figure 44. Stress vs. strain (Trial Mix 3: No GP, long PE for 28 days).

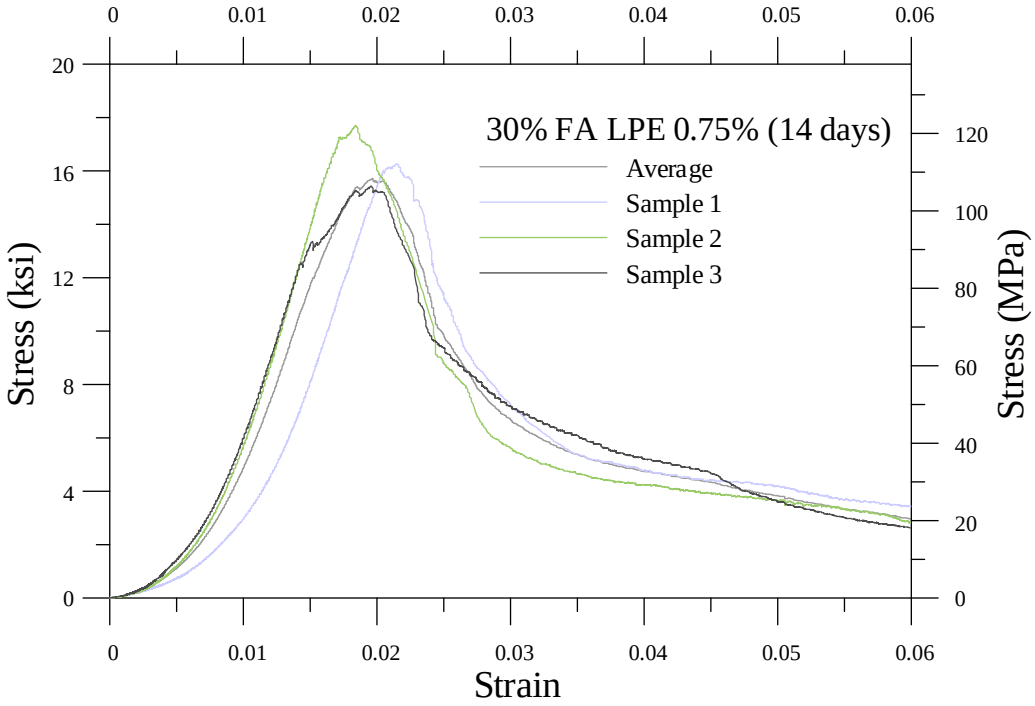

Figure 45. Stress vs. strain (Trial Mix 4: 30% FA, long PE 0.75% for 14 days).

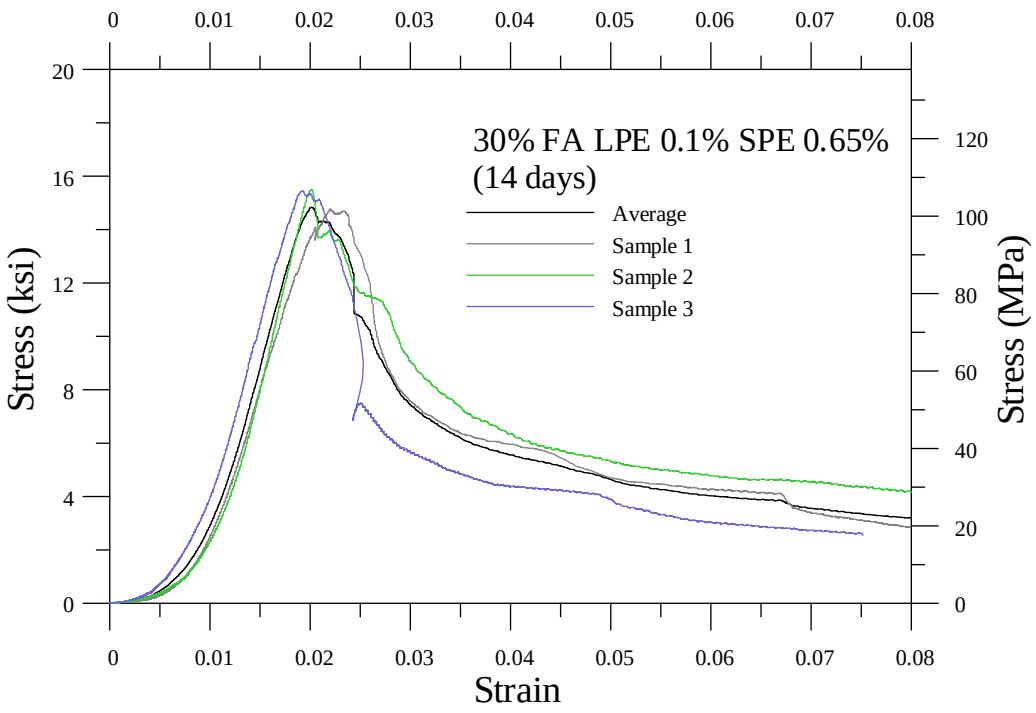

Figure 46. Stress vs. strain (Trial Mix 5: 30% FA, long PE 0.1%, short PE 0.65% for 14 days).

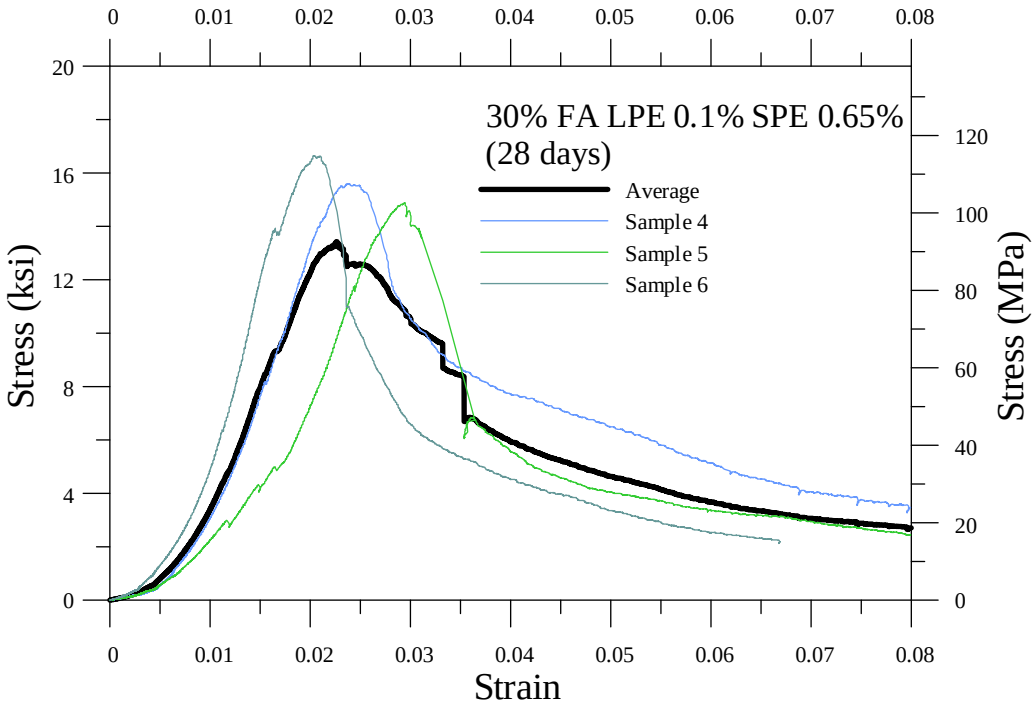

Figure 47. Stress vs. strain (Trial Mix 6: 30% FA long PE 0.1% short PE 0.65% for 28 days).

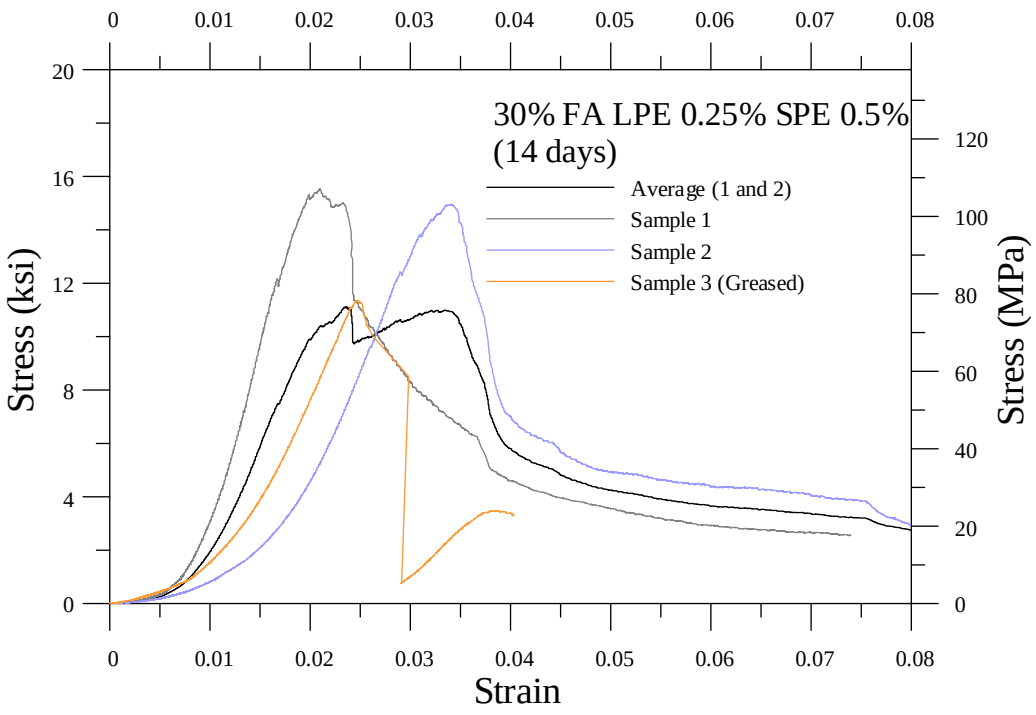

Figure 48. Stress vs. strain (Trial Mix 7: 30% FA long PE 0.25% short PE 0.5% for 14 days).

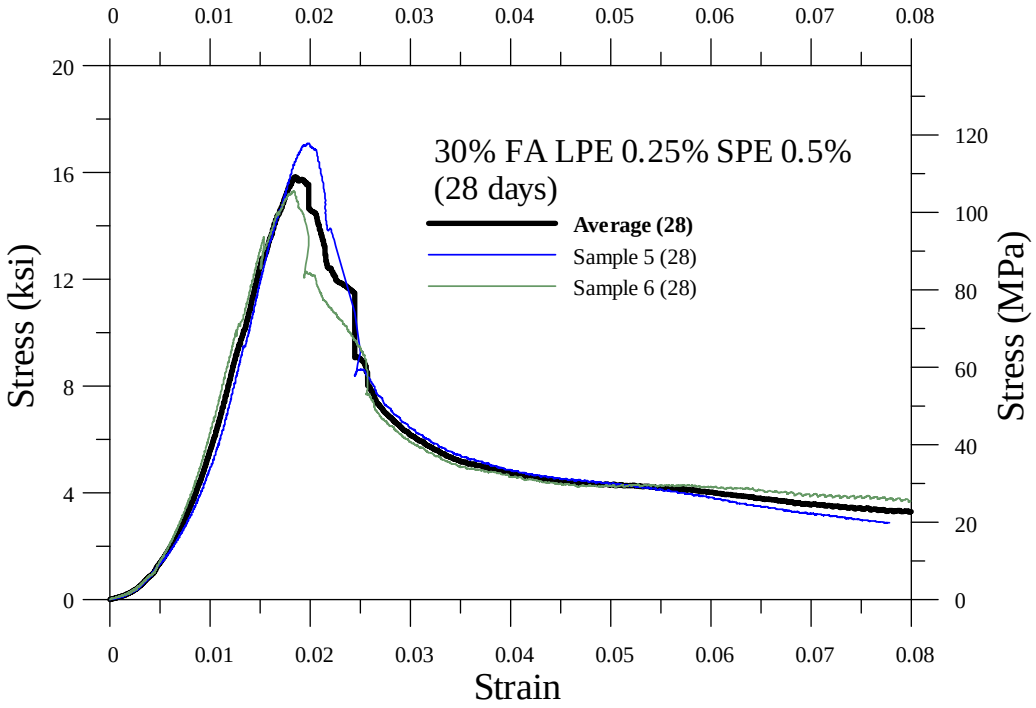

Figure 49. Stress vs. strain (Trial Mix 8: 30% FA long PE 0.25% short PE 0.5% for 28 days).

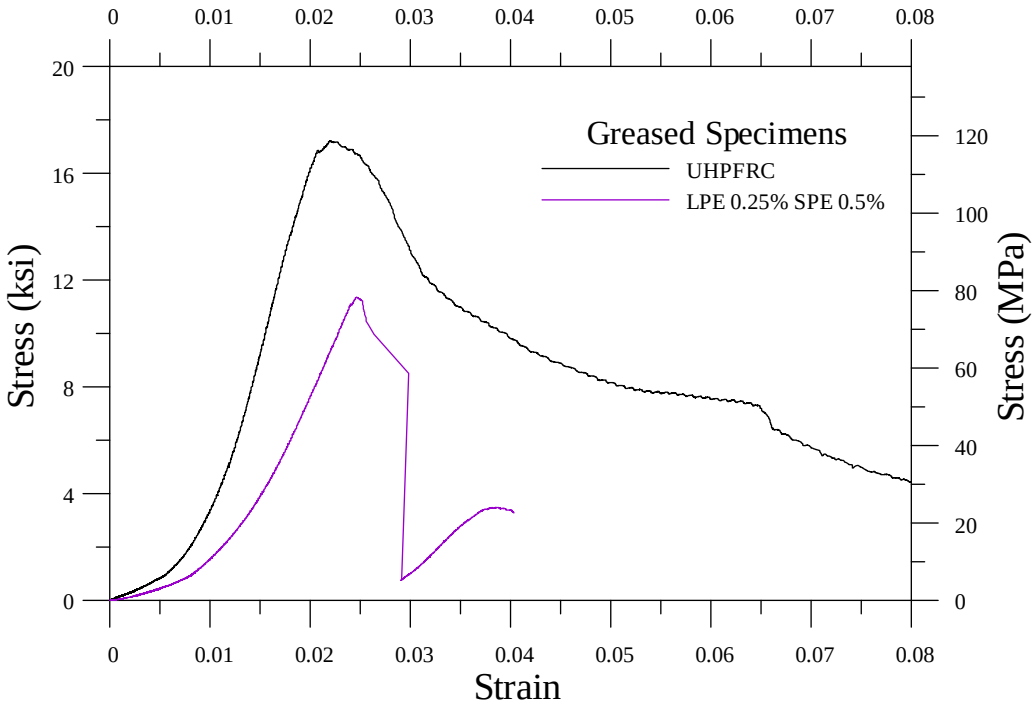

Figure 50. Stress vs. strain (Trial Mix 9 and 11: greased specimens).

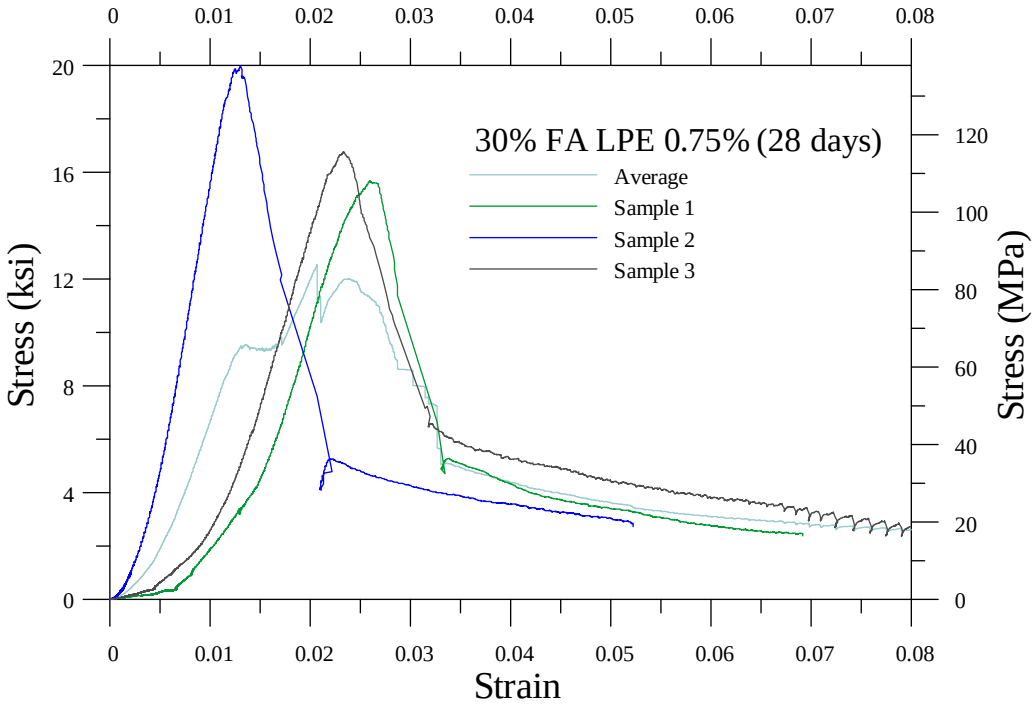

Figure 51. Stress vs. strain (Trial Mix 10: 30% FA long PE 0.75% for 28 days).

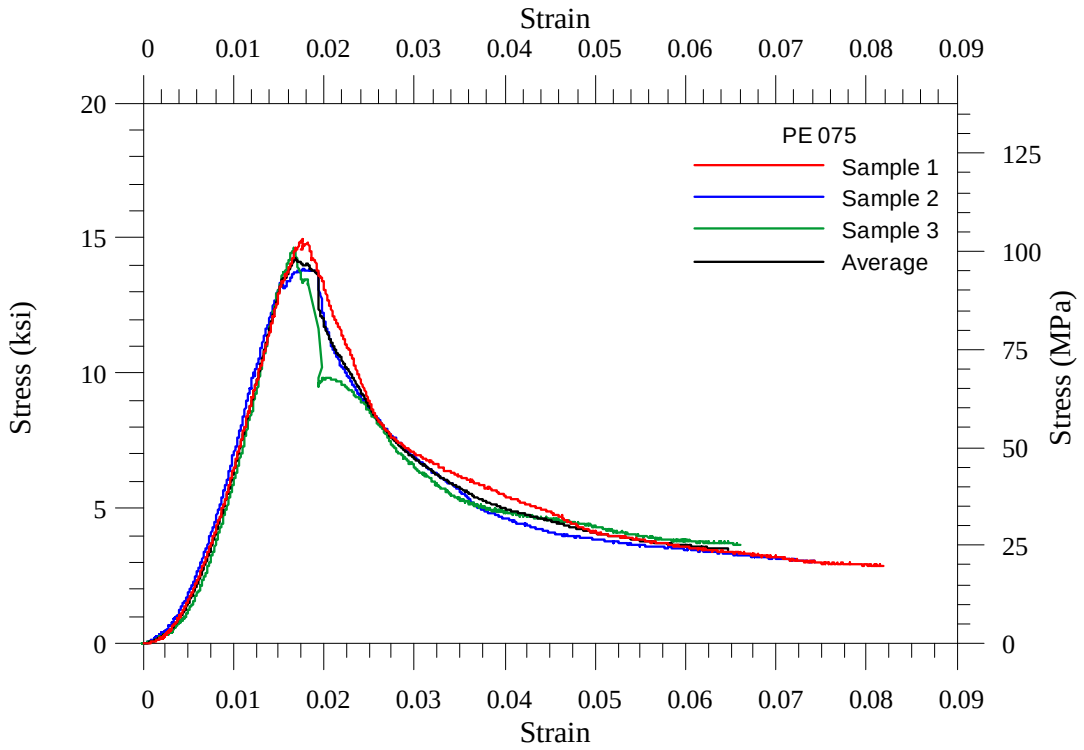

Figure 52. Stress vs. strain (Trial Mix 12: 20% FA PE 0.75%).

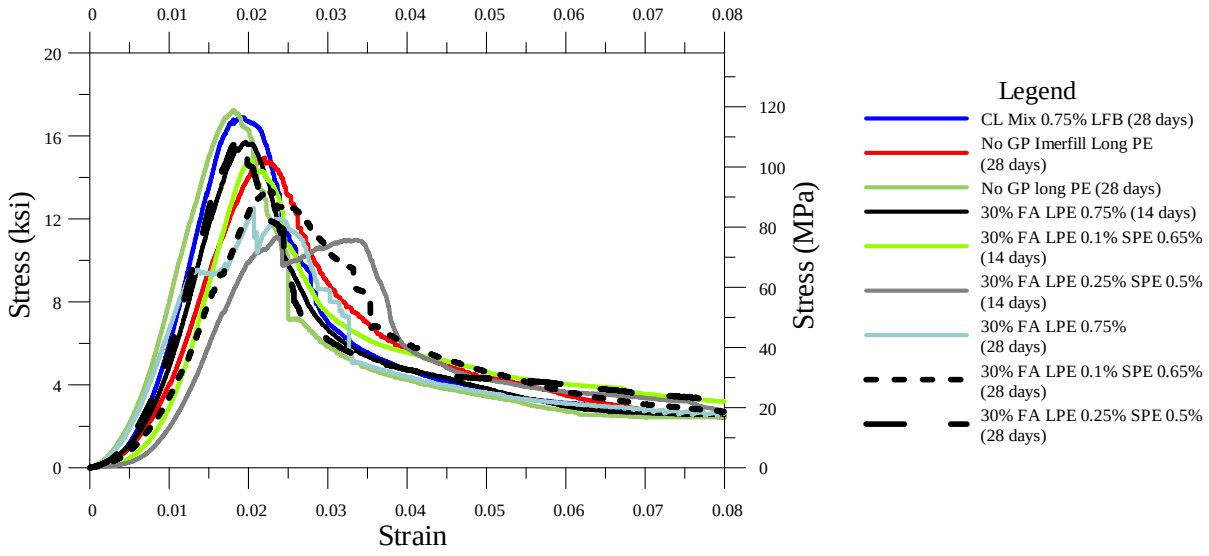

Figure 53. Stress vs. strain (combined).

Among the different mixes that were tried during this phase, based on economics and consistency of the mix, the concrete consisting of 0.75% per unit volume polyethylene fibers was selected. The mix was cured at a temperature of 150 °F and gained a one-day compressive strength of 9.84 ksi. The same UHP-FRC mix was used for the slant shear testing. However, in the UHP-FRC punch test specimen, the heating setup was able to maintain an average temperature of 100 °F. This resulted in a one-day compressive strength of 6.9 ksi.

5.2. Experimental results for Slant Shear Test

A total of 12 slant shear specimens were prepared. However, 5 specimens did not meet the surface roughness criteria and hence the test results were discarded. The slant shear testing information is provided in section 4.2.2 of the report. The test results for the slant shear tests are presented in the Table 5:

Table 5. Slant shear test results.

Specimen Top Half	Days	Peak vertical load (kips)	Shear stress (psi)	Average shear stress (psi)
PC with smooth surface (saw cut)	1	36.6	455	455
PC with surface roughened (roughness level CP7)	1	50.4	625	598
		45.7	570	
PC with #4 rebar and smooth surface (saw cut)	1	44.1	550	609
		52.3	650	
		50.4	625	
UHP-FRC with surface roughened (roughness level CP5)	1	81.9	1019	1019

5.2.1. Strain (PC with Dowel Bars)

Figure 54 shows the vertical applied load versus strain in reinforcement and vertical applied load versus deformation along slip plane obtained from the slant shear test data.

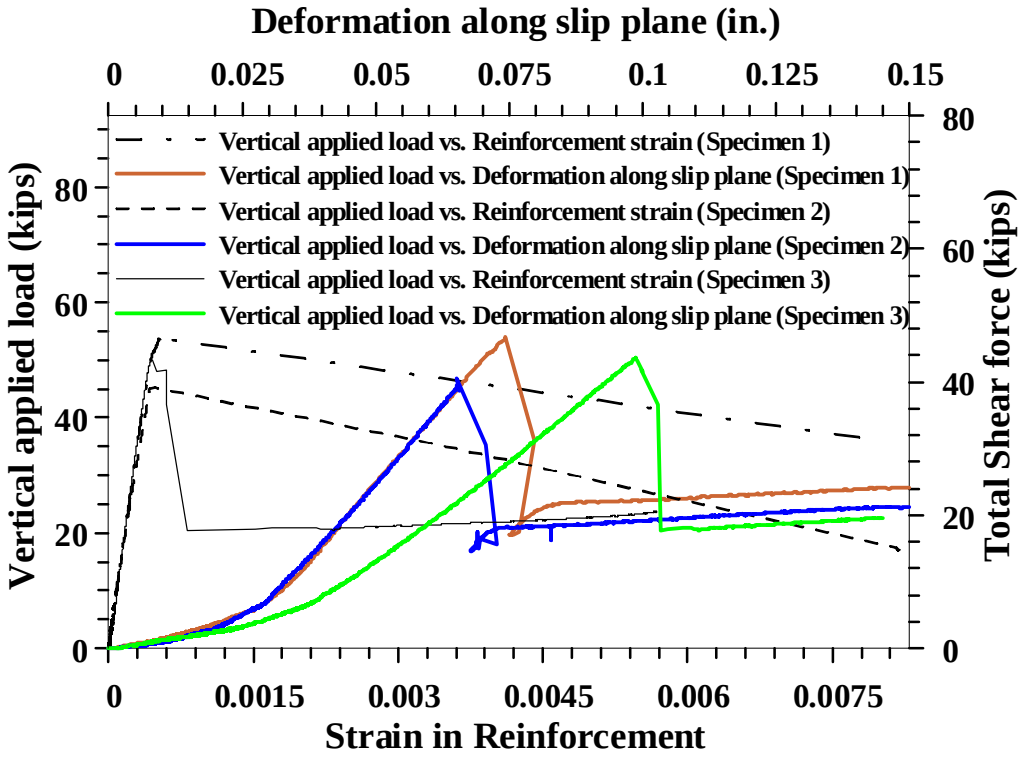

Figure 54. Vertical applied load vs. strain in reinforcement and vertical applied load vs. deformation along the slip plane for SST test specimen with a smooth surface and rebar.

From the graph (Figure 54) above, it was observed that, from Equation 5:

Rebar force = 0.0006 ×29000 ksi × 0.2 in^2 × sin (30°)

= 1.74 kips

This value of rebar force is very low. This suggests that the force developed in the rebar is not very significant at the instant of peak vertical applied load.

5.2.2. UHP-FRC test specimens

The specimens were tested one day after casting of the top half of the slant shear specimen. A pneumatic surface scaler (Figure 55b) was used to approximate ICRI's CSP 5 (Figure 55c) and no dowel bars were used. The UHP-FRC slant shear specimens (Figure 55c) were cured at 150 °F in an oven and after one day, the compressive strength was 10.95 ksi.

For the slant shear specimen, a peak applied vertical load of 81 kips was recorded. This corresponds to a shear force of 71 kips, which is 50% higher than that of conventional pavement repair. A post-test UHP-FRC specimen is shown in Figure 56.

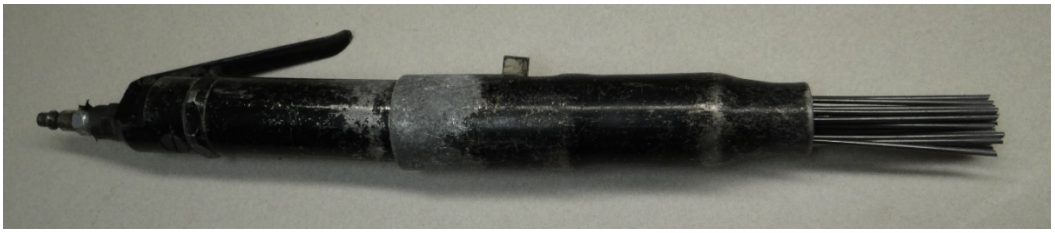

(a)

(b) (c)

Figure 55. (a) A pneumatic needle scaler used to roughen the specimen, (b) roughened surface for the bottom half of the UHP-FRC specimen roughened by using the pneumatic scaler to approximately measure ICRI's CSP 5, and (c) results of the UHP-FRC slant shear test.

(a) (b)

Figure 56. Post-test pictures of slant shear specimen. (a) Lower part: plain concrete and (b) Upper part: UHP-FRC.

5.2.3. Main Findings

The following are the findings of the slant shear tests:

- From the slant shear tests, it was observed that the peak shear stress for UHP-FRC is 167% of the shear stress recorded for the Portland cement concrete (PCC). Hence, UHP-FRC shows a significantly better interface bond strength than PCC.
- For the slant shear specimen with a smooth interface embedded with a No. 4 dowel bar, it is seen that the strain in the rebar is significantly lower when the peak value of the vertical load is reached. The strain in the rebar increased gradually and then yielded after the peak vertical load was achieved. This implies that the rebar does not contribute to bond strength development at peak load.
- The peak vertical load values for the PC does not show much variation for different levels of concrete surface preparation. Previous research carried out using large scale push off tests *(18, 19)* with various magnitudes of surface roughness indicated that a rougher surface can provide strong interface shear resistance. This contradicts the data obtained from the slant shear test. Hence, a different test method is necessary for accurate representation of the interface bond strength between the existing concrete and the new repair concrete. For this purpose, further test results are necessary using the punch tests to determine the exact values of shear strength.

5.3. Experimental Results for Punch Test

The results of the punch test are summarized in the Table 6 below:

Table 6. Results for punch test specimens.

Punch specimen	Peak applied vertical load (kips)	Vertical deformation at peak (in)	Shear stress (psi)	Remarks
PC with dowel bars and interface surface smooth	39.3	0.027	120	-
UHP-FRC without dowel bars and interface roughness CSP 5	51.3	0.054	160	30% more

5.3.1. Observed Cracking (PC with Dowel Bars)

The specimen reached a peak load of 39.3 kips at a vertical deformation of 0.027 in. The loading behavior is shown in the Figure 41. The nature of the vertical load vs. vertical deformation and vertical load vs reinforcement strain obtained is similar to the nature of the graph obtained from the slant shear tests. The loading curve shows no development of strain in the rebar at the peak load. The graph shows a significant drop in the vertical applied load after the peak. The load then increases gradually in proportion to the increase in reinforcement strain till the rebar yields, which is followed by the sudden drop in the load. The vertical deformation corresponding to the drop in the load by the yielding of rebar is 0.1 inch.

The vertical applied load vs strain of reinforcement is represented by the dashed line and the vertical applied load vs vertical deformation is represented by the solid line in Figure 57 shown below.

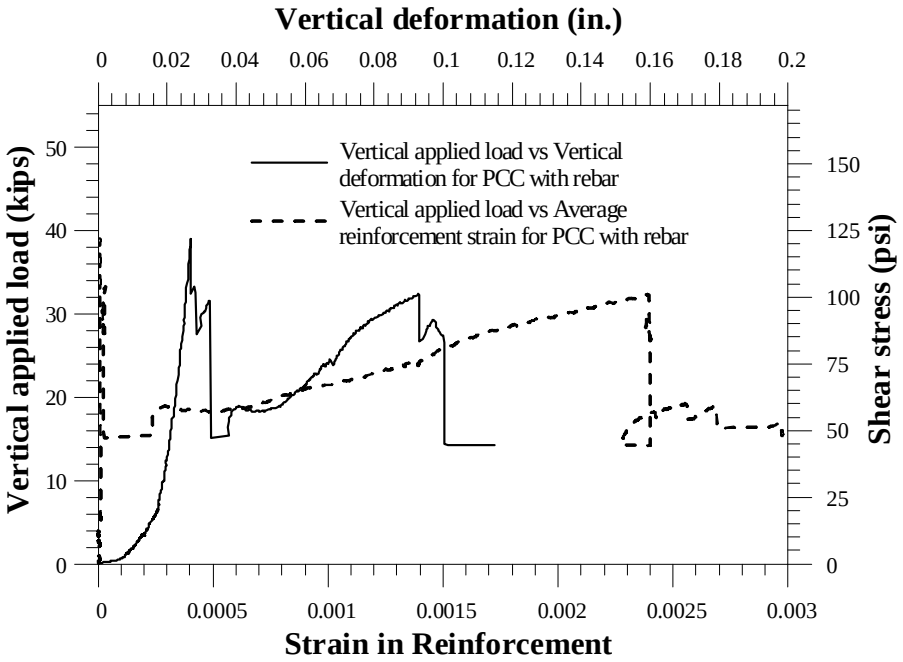

Figure 57. Vertical applied load vs strain in reinforcement and vertical applied load vs. vertical deformation for PC concrete repair with dowel bars.

The following figures (Figure 58 to 62) show the test specimen before and after the completion of the tests.

Figure 58. Punch test setup for PC specimen with dowel bars.

Figure 59. Cracks observed at the interface between repair cast in place PC and the old concrete (outer hollow slab) post peak.

Figure 60. Cracks seen in the outer slab initiating from the interface with the loading plates.

Figure 61. Cracks seen at mid-span of the longer dimension extending throughout the depth of the slab.

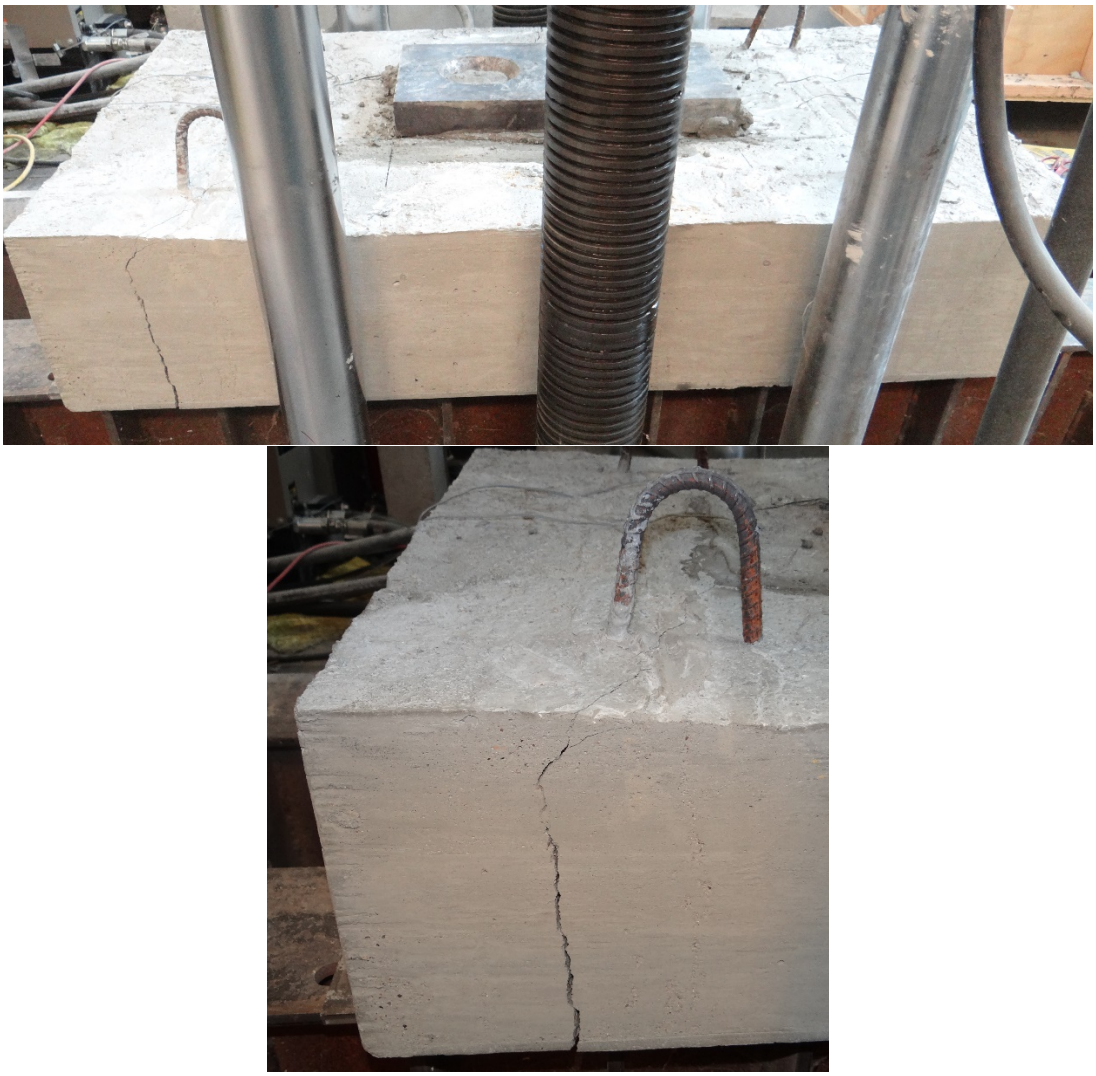

Figure 62. Throughout cracks observed near the slab ends propagating from the corner of the inner slabs.

5.3.2. Observed Cracking (UHP-FRC)

The specimen reached a peak vertical load of 51.3 kips at a vertical deformation of 0.054 in. The specimen maintained the peak vertical load until a vertical deformation of 0.1 in. was reached. It was then followed by a gradual decrease in the vertical applied load with an increase in vertical deformation. No cracks were observed before the peak vertical load was reached.

Figure 63 presents the vertical applied load vs. vertical deformation for the UHP-FRC punch specimen.

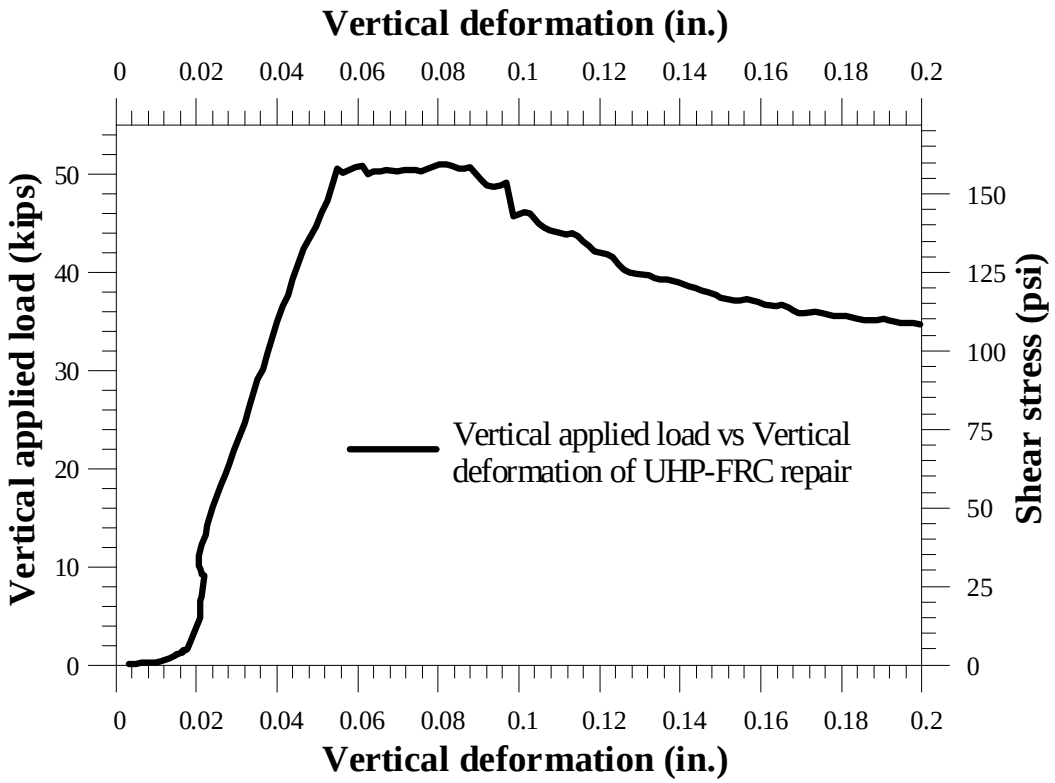

Figure 63. Vertical applied load vs. vertical deformation of UHP-FRC punch test specimen.

Figures 64 – 69 show the test specimen before and after the completion of the tests.

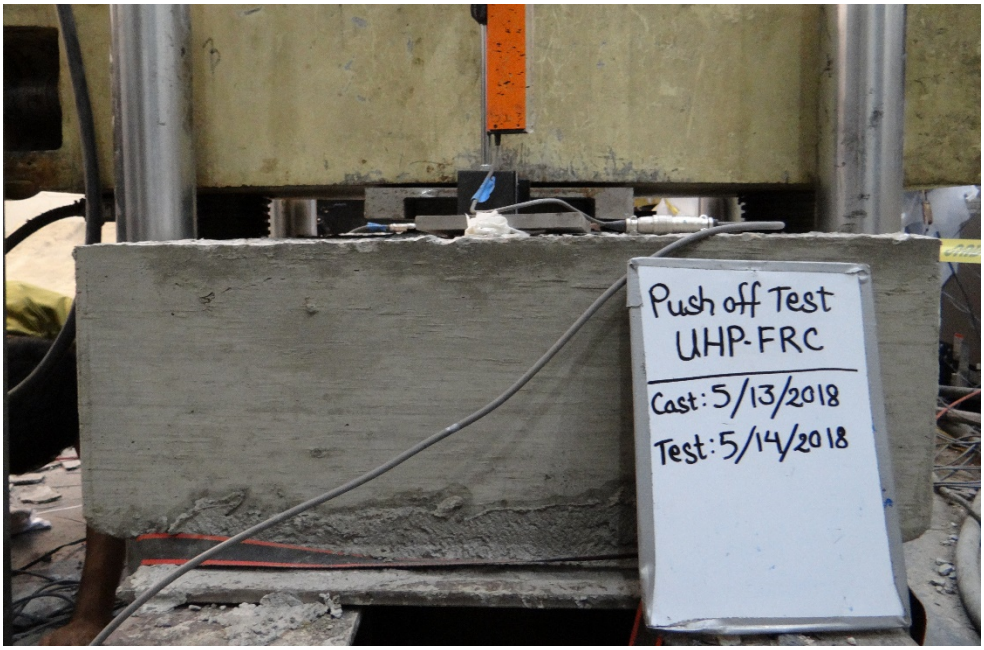

Figure 64. Punch test setup for specimen with UHP-FRC precast slab and cast-in-place joint.

Figure 65. Interface cracks observed in the UHP-FRC punch test specimen after peak.

Figure 66. Initiation of cracks from the corner of the repair joint at 44 kips of the post peak vertical load.

Figure 67. Interface crack caused due to vertical slip and cracks observed on the outer support slab.

Figure 68. Vertical deformation of the central repair slab and cracks propagating from the corner of the repair slab into the supporting outer slab.

Figure 69. Cracks at the mid-span and the edge of the support outer slab.

5.3.3. Main Findings

The following are the finding of the punch test:

- The No. 4 dowel bars showed no strain when the peak vertical load was reached. This implies that the dowel bars had no contribution to the interface bond strength unless significant interface slip was reached.
- The UHP-FRC punch test specimen consisting of precast UHP-FRC panels and a cast-in-place UHP-FRC joint shows 30% greater peak vertical load than that of the cast-in-place PC punch test specimen with dowel bars.
- The PC punch test specimen exhibits a rapid strength drop (Figure 57) after reaching the peak load while the UHP-FRC specimen maintained the peak vertical load up to a significant vertical deformation followed by a gradual decrease in the load. This ductility allows force redistribution in the actual pavement should the load exceed the capacity of the UHP-FRC strip used for repair.
- The outer hollow slab was not reinforced and showed significant cracking during the test.

5.4. Life-Cycle Cost Analysis, Field Installation and Performance Monitoring

5.4.1. Life-cycle Cost Analysis (LCCA)

The life-cycle cost of cast in place (CIP) concrete pavement repair is compared with the proposed ultra-high- performance fiber-reinforced concrete (UHP-FRC) pavement repair.

The considerations considered while performing the LCCA are presented below:

- Panel thickness of 10 in. for both the scenarios were considered.
- Days required for each section in construction scheduling for CIP pavement repair was taken to be 7 days and 1 day for UHP-FRC pavement repair (similar to precast pavement repair) for every component. *(32)*
- The lane being repaired was closed for the entire duration of the scheduled pavement repair process.

- The user cost associated was assumed to be constant throughout the analysis period for simplicity.
- The LCCA was performed on a single lane (width of 12 ft and depth of 10 in.) for 1-mile length.
- Material cost for CIP pavement repair was taken as $250/yd^3$.
- Material cost for UHP-FRC pavement repair was taken as $1500/yd^3$.
- Maintenance strategy of CIP concrete pavement repair *(33)* was used. The maintenance interval for UHP-FRC repair was taken as double than the CIP concrete pavement repair owing to its increased durability.
- A 100 years analysis period was taken.
- Total cost for cast in place pavement repair was taken as $917,123 per lane mile (1997-2001 data form INDOT Contracts Division).
- Work zone cost and circuitry costs from the FHWA Interim Technical Bulletin *(34)* were used after some modifications.
- Crash costs were ignored to simplify the calculations.
- The annual traffic growth rate for the analysis period was assumed to be 3%.

Calculation Data and Graphs: The calculated agency costs and user costs associated with the conventional cast in place concrete pavement repair and the proposed UHP-FRC pavement repair method are presented in the Table 7.

The data for the conventional CIP concrete repair in the Table 7 are converted to net present values for a varying discount rates starting from 1% to 6% with 1% increments and are presented in the Table 8.

The data for the proposed UHP-FRC pavement repair in the Table 7 are converted to net present values for a varying discount rates starting from 1% to 6% with 1% increments and are presented in the Table 9.

Table 7. The agency and user costs associated with the CIP concrete pavement repair and the proposed UHP-FRC pavement repair method.

Years	CIP			UHP-FRC		
	Agency cost	User cost	Sum	Agency cost	User cost	Sum
	×1000	×1000	×1000	×1000	×1000	×1000
0	$917	$313	$1,230	$2,995	$45	$3,039
10	$64	$421	$485			
20				$64	$81	$145
15	$92	$488	$580			
25	$92	$656	$748			
30				$92	$109	$201
35	$92	$881	$974			
40	$64	$1,022	$1,086			
45	$92	$1,184	$1,277			
50	$917	$1,373	$2,290	$92	$196	$289
60	$64	$1,845	$1,909			
65	$92	$2,139	$2,232			
70				$92	$354	$447
75	$92	$2,875	$2,967			
80				$64	$476	$540
85	$92	$3,864	$3,956			
90	$64	$4,479	$4,543	$92	$640	$732
95	$92	$5,193	$5,285			
100	$0	$0	$0	$0	$0	$0

Table 8. Net present value with varying discount rates for CIP pavement repair

Years	Total cost ×1000	NPV ×1000					
		i=1%	i=2%	i=3%	i=4%	i=5%	i=6%
0	$1,230	$1,230	$1,230	$1,230	$1,230	$1,230	$1,230
10	$485	$485	$398	$361	$328	$298	$271
15	$580	$476	$431	$373	$322	$279	$242
25	$748	$645	$456	$357	$281	$221	$174
35	$974	$722	$487	$346	$247	$177	$127
40	$1,086	$766	$492	$333	$226	$154	$106
45	$1,277	$858	$524	$338	$219	$142	$93
50	$2,290	$1,464	$851	$522	$322	$200	$124
60	$1,909	$1,161	$582	$324	$181	$102	$58
65	$2,232	$1,228	$616	$327	$174	$94	$51
75	$2,967	$1,479	$672	$323	$157	$76	$38
85	$3,956	$1,785	$735	$321	$141	$63	$28
90	$4,543	$1,950	$764	$318	$133	$56	$24
95	$5,285	$2,158	$805	$319	$127	$51	$21
100	$0	$0	$0	$0	$0	$0	$0
	Total x 1000	$16,406	$9,043	$5,791	$4,089	$3,143	$2,586

Table 9. Net present value with varying discount rates for UHP-FRC pavement

Years	Total cost ×1000	NPV ×1000					
		i=1%	i=2%	i=3%	i=4%	i=5%	i=6%
0	$3,039	$3,039	$3,039	$3,039	$3,039	$3,039	$3,039
20	$145	$119	$97	$80	$66	$55	$45
30	$201	$149	$111	$83	$62	$47	$35
50	$289	$175	$107	$66	$41	$25	$16
70	$447	$223	$112	$56	$29	$15	$8
80	$540	$244	$111	$51	$23	$11	$5
90	$732	$299	$123	$51	$21	$9	$4
100	$0	$0	$0	$0	$0	$0	$0
	Total x1000	$4,248	$3,701	$3,426	$3,281	$3,200	$3,152

The net present values for corresponding values of discount rates for the conventional CIP pavement repair method and proposed UHP-FRC pavement repair are summarized and compared in the Table 10 below.

Table 10. Comparison of results of LCCA between CIP concrete pavement repair and proposed UHP-FRC repair for varying discount rates for the 100-year analysis period.

Discount rate	CIP concrete pavement repair	Proposed UHP-FRC pavement repair	Remarks
i%	Total × 1000	Total × 1000	
1%	$16,406	$4,248	26%
2%	$9,043	$3,701	41%
3%	$5,791	$3,426	59%
4%	$4,089	$3,281	80%
5%	$3,143	$3,200	102%
6%	$2,586	$3,152	122%

The above table 10 is presented in a graphical format in the Figure 70 below.

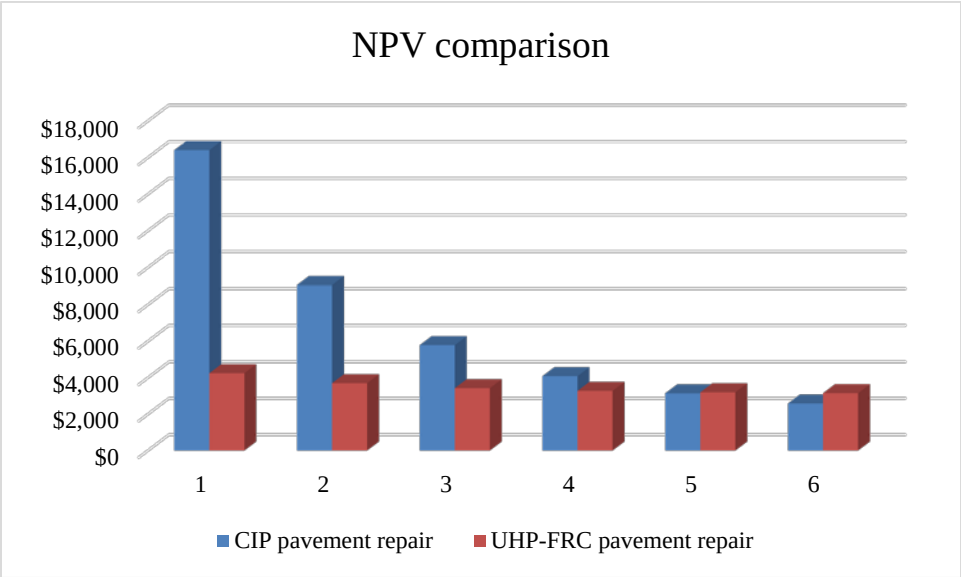

Figure 70. Comparison of net present value of the two alternatives; the horizontal axis represents the discount rate in percentage and the vertical axis represents the net present value in thousands (× 1000).

Findings:

The findings of the LCCA are presented below:

- It was observed that the initial construction cost of the proposed UHP-FRC pavement repair method was higher than the CIP pavement repair method.
- The conventional CIP pavement repair method employs maintenance activities at shorter intervals as compared to the UHP-FRC pavement repair method. This results in an increased user costs during the analysis period for the conventional CIP concrete pavement repair method. Also, the shorter construction time for the UHP-FRC pavement repair method (1 day) further reduces the user costs.
- For low values of discount rates (<5%), the net present value of the conventional CIP pavement repair method is higher than the proposed UHP-FRC pavement repair method.

5.4.2. Field Installation

The idea of using sustainable UHP-FRC for pavement repair was done in a pilot installation in the City of Bedford, Texas with the assistance from Bedford Public Works. They intended to try on-site casting of UHP-FRC rather than the precast one, so the only difference is the material and keeping the procedure the same as the traditional method (that is, continued to use dowel bars). Therefore, the UTA research team rented special high-shear mixers and brought all the materials and mixed UHP-FRC on site (Figure 71). This led to consideration of other spots to use the precast method as developed in the recent project.

Figure 71. Field installation in the City of Bedford, TX.

5.4.3. Performance Monitoring

The location for the proof-of-concept UHP-FRC pavement implementation plane at the Dallas-Fort Worth International Airport will be at the apron connected to Taxiway of the American Airlines Aircraft Maintenance Hangar. A long-term monitoring will be conducted to inspect any internal damage in the pavement due to heavy aircraft loads. Two non-destructive testing (NDT) methods, acoustic scanning system using acoustic rolling impactor (ARI) and advanced post processing system of ground penetrating radar (GPR), will be used to image the UHP-FRC pavement. These two systems have been used at the Arlington Municipal Airport by UTA researchers.

6. CONCLUSIONS

The conclusions drawn from data collected during this research are presented below:

1. Conventional concrete pavement repair uses a saw cut to remove the damaged portion and leaves a smooth surface at the cut surface. It then uses dowel bars to engage the new and existing concrete pavement to transfer the force and prevent faulting between the interface; however, experimental tests showed that the rebars used as dowel bars to prevent faulting do not play a major role in the interface load transfer at the peak load. A certain vertical deformation of the pavement (i.e., damage or faulting) is required before the rebar can start carrying the load. From this observation it can be concluded that the replacement of dowel bars by a roughened interface is feasible. This research showed that using a roughened surface (up to CSP4 or CSP 5) provides a very large bond resistance which is enough to prevent faulting. Replacing dowel bars by roughening the surface can eliminate the preparation time for dowel bars (drilling holes and waiting epoxy to harden). While drilling holes takes may take less time than that for roughening the surface, the curing time for epoxy can take several hours.
2. The slant shear test overestimates the shear capacity due to the influence of a frictional force resulting from the normal component of the applied vertical force (Table 5). As a result, a new test, the punch test, was developed in this research to obtain a more realistic shear capacity of the interface.
3. From the peak load values obtained from the slant shear test and the punch test, the bond strength of UHP-FRC is substantially greater than plain concrete.
4. A new method for concrete repair was developed and is proposed, which combines the features of precast UHP-FRC with cast-in-place repair of pavement without any dowel bars (Figure 23). In this method, a precast UHP-FRC panel is used along with cast-in-place UHP-FRC. The vertical repair surfaces of the existing concrete are roughened on site. The outer edges of the UHP-FRC precast slabs are roughened before they are brought to the site (no dowel bars are needed). The depth of the precast UHP-FRC is the same as the existing pavement slab thickness. Only a small cast-in-place UHP-FRC joint (one to two inches wide) is done onsite. The roughened precast UHP-FRC slab is placed in the repair area and UHP-FRC is cast in the joint.
5. This proposed method has several advantages over the conventional repair methods: (1) pavement reconstruction using precast panels need only overnight closures, compared with a long-term closure for conventional methods *(31)*; (2) The largest portion of the repair is precast, which provides higher quality control than cast-in-place concrete; (3) a limited amount of cast-in-place UHP-FRC is used and dowel bars are eliminated, which reduces the work and labor, as well as the downtime; 4) UHP-FRC can gain high early strength in a few hours, which can accelerate the repair work.
6. From the LCCA it can be concluded that although the initial capital cost of the proposed UHP-FRC pavement repair method is higher than the cast-in place pavement repair method, using the UHP-FRC pavement repair method can be much cost-effective when life-cycle period is considered.

7. RECOMMENDATIONS

The recommendations from this study are:

1. The UHP-FRC mixes (obtained from trial testing) were able to reach a high early strength. A one-day compressive strength is approximately 10 ksi. Also, the mix with 0.75% by volume of ultra-high molecular weight polyethylene (PE) fibers provided a consistent strength. Hence, the ratio of 0.75% by volume is recommended.
2. During the trial mixing it was observed that a curing temperature of 150 °F resulted in higher early strength gain of the UHP-FRC. Temperature curing is recommended for the cast-in-place UHP-FRC joints should a high early compressive strength, such as 2500 psi, is needed within 4 to 5 hours.
3. A large-scale proof-of-concept test for an actual pavement replacement or repair is recommended to identify any potential onsite problems that a contractor may have. This test can facilitate the wide applications of the proposed sustainable pavement repair method.

REFERENCES

1. Mehta, P. K. and Monteiro, P. J. M., Concrete—Microstructure, Properties, and Materials, Fourth edition, McGraw-Hill, 2014.

2. Graybeal, B., and Tanesi, J., “Durability of an Ultra-High-Performance Concrete,” Journal of Materials in Civil Engineering, Vol. 19, No. 10, pp. 848-854, 2007.

3. Horii, H. and Nemat-Nasser, S., “Compression-Induced Microcrack Growth in Brittle Solids: Axial Splitting and Shear Failure,” Journal of Geophysical Research, Vol. 90, No. B4, pp. 3105-3125, 1985.

4. Chao, S.-H. (2008), "Achieving “Green” Concrete through the Use of High Performance Fiber Reinforced Concrete," ASCE Texas Section Fall Meeting, Addison, Dallas, October 3rd, 2008.

5. Roesler, J. R., Hiller J. E., Brand, A.S. Continuously Reinforced Concrete Pavement Manual Guidelines for Design, Construction, Maintenance, and Rehabilitation. Report FHWA-HIF-16-026. FHWA, U.S. Department of Transportation, August 2016.

6. Pavement Tools Consortium; “pavementinteractive.org”, 2018.

7. AASHTO Guide for Design of Pavement Structures. American Association of State Highway and Transportation Officials, Washington, D.C., 1993, pp. III-59 – III-78.

8. AASHTO Guide for Design of Pavement Structures 1993 (vol. 1), ISBN-13: 978-1560510550. American Association of State Highway and Transportation Officials, Washington, D.C., 1993

9. American Concrete Pavement Association. Guidelines for Full-Depth Repair. Technical Bulletin TB002.0[4]2P. ACPA, Skokie, IL, 1995.

10. Concrete Pavement Rehabilitation and Preservation Treatments. TechBrief. No. FHWA-IF-06-005. FHWA, US Department of Transportation, 2005.

11. Stacks, D. L. Pavement Manual. Manual Notice 2018-1. TxDOT Online Manual, May 01, 2018.

12. Rapid Construction of Rigid (Portland Cement Concrete) Airfield Pavements. Advisory circular No: 150/5370-16. FAA, U.S. Department of Transportation, September 28, 2007.

13. Van Dam, T. J.,Peterson, K. R., Sutter, L. L., Panguluri A., Sytsma, J., Buch, N., Kowli, R., and Desaraju, P. Early-Opening-to-Traffic Portland Cement Concrete for Pavement Rehabilitation. NCHRP Web Document 76. National Cooperative Highway Research Program, Washington, DC, 2005.

14. Tayabji, S., Ye, D., and Buch, N. “Precast concrete pavements: Technology overview and technical considerations”, PCI Journal, Vol. 58, Issue 1, Winter 2013, pp. 112-128.

15. Ahlborn, T., Harris, D., Misson, D., and Peuse, E. (2011), “Characterization of Strength and Durability of Ultra-High-Performance Concrete Under Variable Curing Conditions,”

Transportation Research Record: Journal of the Transportation Research Board, No. 2251, Transportation Research Board of the National Academies, Washington, D.C., 2011, pp. 68–75. DOI: 10.3141/2251-07.

16. Aghdasi, P., Heid A. E., and Chao, S.-H. (2016), "Developing Ultra-High-Performance Fiber-Reinforced Concrete for Large-Scale Structural Applications," ACI Materials Journal, V. 113, No. 5, September-October 2016, pp. 559-570.

17. Kaka, V. B. "Applications of Ultra-High Performance Fiber-Reinforced Concrete on Flexural Structural and Architectural Members.", Master Thesis, Department of Civil Engineering, University of Texas at Arlington, TX, 2017, 348 pp.

18. Palacios, G. "Performance of Full-Scale Ultra-High Performance Fiber-Reinforced Concrete Column Subjected to Extreme Earthquake-Type Loading and Effect of Surface Preparation on the Cohesion and Friction Factors of the AASHTO Interface Shear Equation." Master Thesis, Department of Civil Engineering, University of Texas at Arlington, TX, 2015, 625 pp.

19. Waweru, R. N. "Strength of Horizontal Shear Reinforcement with Limited Development." Ph.D. Dissertation, University of Texas at Arlington, Arlington, TX, 2015. 305 pp.

20. Khayat, K. H. and Valipour, M. (2014), "Design of Ultra High Performance Concrete as an Overlay in Pavements and Bridge Decks," Center for Transportation Infrastructure and Safety/NUTC program, Missouri University of Science and Technology, funded by U.S. Department of Transportation Research and Innovative Technology Administration, 2014.

21. Muñoz, M. A. C. "Compatibility of Ultra High Performance Concrete as Repair Material: Bond Characterization with Concrete under different Loading Scenarios." Master Thesis, Department of Civil Engineering, Michigan Technological University, 2012.

22. Shann, S. V. "Application of Ultra High Performance Concrete (UHPC) as a Thin Bonded Overlay for Concrete Bridge Decks." Master Thesis, Department of Civil Engineering, Michigan Technological University, 2012.

23. Sarkar, J. "Characterization of the Bond Strength between Ultra High Performance Concrete Bridge Deck Overlays and Concrete Substrates." Master Thesis, Department of Civil Engineering, Michigan Technological University, 2010.

24. Hadl, P., Pietra R. D., Hoang, K. H., Pilch, E., Tue, N. V. "Anwendung von UHPC als direkt befahrener Aufbeton bei der Integralisierung eines bestehenden Brückenbauwerks in Österreich." Ernst & Sohn Verlag für Architektur und technische Wissenschaften GmbH & Co. KG, Berlin. Beton- und Stahlbetonbau 110 (2015), Heft 2.

25. Buitelaar, P., "Heavy Reinforced Ultra High Performance Concrete," Proceedings of the International Symposium on Ultra High Performance Concrete, Ed., Schmidt, M., Fehling, E., and Geisenhanslüke, C., Kassel University Press, Kassel, Germany, 2004, pp. 25–35.

26. Yuguang, Y., Walraven, J., and den Uijl, J., "Study on Bending Behavior of an UHPC Overlay on a Steel Orthotropic Deck," *Proceedings of the Second International Symposium on*

Ultra High Performance Concrete, Ed., Fehling, E., Schmidt, M., and Stürwald. S., Kassel University Press, Kassel, Germany, 2008, pp. 639–646.

27. Sajna, A., Denarié, E., and Bras, V., "Assessment of a UHPFRC Based Bridge Rehabilitation in Slovenia, Two Years After Application," *Proceedings of Hipermat 2012 3rd International Symposium on UHPC and Nanotechnology for High Performance Construction Materials*, Ed., Schmidt, M., Fehling, E., Glotzbach, C., Fröhlich, S., and Piotrowski, S., Kassel University Press, Kassel, Germany, 2012, pp. 937–944.

28. Russell, H. G., Graybeal, B. A., Ultra-High Performance Concrete: A State-of-the-Art Report for the Bridge Community. Report FHWA-HRT-13-060. FHWA, U.S. Department of Transportation, June 2013.

29. ASTM. "Standard Test Method for Bond Strength of Epoxy-Resin Systems Used with Concrete by Slant Shear1." C882/C882M − 13a, ASTM International, 2013, 4 pp.

30. Santos, P. M. D. "Assessment of the Shear Strength between Concrete Layers." Ph.D. Dissertation, University of Coimbra, July. 2009. 338 pp.

31. Switzer, W. J., Fischer, A., Fuselier, G. K., Smith, P. J. and Verfuss, W. "Overnight Pavement Replacement Using Precast Panels and Conventional Subgrade Material, Washington Dulles International Airport Case Study," Airfield Pavement Specialty Conference (ASCE), pp. 259 – 278, 2003.

32. Menard, R. Why Precast Costs Less. Precast Magazine, National Precast Concrete Association, May. 2010. Accessed November 05, 2018.

33. Pennsylvania Department of Transportation, Publication 242 Pavement Policy Manual, February. 2018.

34. Walls III, J. and Smith, M. R. Life-Cycle Cost Analysis in Pavement Design-Interim Technical Bulletin. FHWA-SA-98-079. FHWA, U.S. Department of Transportation, September 1998.